



## An uncertain future for the climate and health impacts of anthropogenic aerosols in Africa

Joe Adabouk Amooli<sup>1</sup>, Marianne T. Lund<sup>2</sup>, Sourangsu Chowdhury<sup>2</sup>, Gunnar Myhre<sup>2</sup>, Ane N. Johansen<sup>2</sup>, Bjørn H. Samset<sup>2</sup>, and Daniel M. Westervelt<sup>1,3</sup>

5 <sup>1</sup>Lamont-Doherty Earth Observatory, Columbia University, New York, NY, United States of America

<sup>2</sup>CICERO Center for International Climate Research, Oslo, Norway

<sup>3</sup>NASA Goddard Institute for Space Studies, New York, NY, United States of America

**Correspondence to:** Daniel M. Westervelt, danielmw@ldeo.columbia.edu

### 10 **Abstract**

Limited data availability and distinct regional characteristics of sources lead to a wide range of future aerosol emissions projections for Africa. Here we quantify and explore the implications of this spread for climate and health impact assessments. Using the Evaluating the Climate and Air Quality Impacts of Short-Lived Pollutants (ECLIPSE), the Shared Socioeconomic Pathways (SSPs), and the United Nations Environment Programme (UNEP) emission projections, we find high scenario diversity and regional heterogeneity in projected air pollution emissions across sub-Saharan Africa. Using 10 different emissions pathways as input to the Oslo chemical transport model version 3 (OsloCTM3), we find that regionally-averaged annual-mean population-weighted PM<sub>2.5</sub> concentrations exhibit divergent trends depending on scenario stringency, with Eastern Africa PM<sub>2.5</sub> concentrations increasing by up to 6 µg m<sup>-3</sup> (37 %, SD ± 2.7 µg m<sup>-3</sup>) by 2050 under the UNEP Baseline, SSP370, and ECLIPSE current legislation scenarios. In almost all cases, there is a substantial increase in the number of excess deaths, with increases of up to more than 2.5 times compared to the baseline. We also find a net positive aerosol-induced radiative forcing across sub-Saharan Africa in all scenarios by 2050 except two high-sulfur emission UNEP scenarios, with values ranging from 0.03 W m<sup>-2</sup> in SSP119 to 0.27 W m<sup>-2</sup> in SSP585. The wide spread in projected emissions and differences in sectoral distributions across scenarios highlights the critical need for accurate activity data and harmonization efforts in preparation for upcoming assessments such as the 7th Assessment Report of the Intergovernmental Panel on Climate Change.



## 30      **1. Introduction**

Emissions of anthropogenic aerosols, their precursors, and reactive gases are projected to undergo substantial changes in the coming decades, having a major impact on climate and air quality (Lund et al., 2019; Westervelt et al., 2020). In the United States (U.S.) and Europe, sulfur dioxide (SO<sub>2</sub>), black carbon (BC), and organic aerosol (OA) emissions have been declining in recent decades (Leibensperger et al., 2012; Westervelt et al., 2015). In contrast, emissions have significantly increased in Africa and other countries in the Global South in recent decades (Fontes et al., 2017; Samset et al., 2019; Wang et al., 2023). In major emitting regions, aerosol-induced cooling has offset up to 1°C of surface warming since the pre-industrial era (Samset et al., 2019), and the sensitivity of regional climates to reductions in aerosol emissions is high (Samset et al., 2018; Westervelt et al., 2020). Aerosols impact surface temperature not only by directly scattering or absorbing incoming solar radiation but also indirectly by altering cloud properties, including their brightness and lifespan (Albrecht, 1989; Twomey and S., 1977). Changes in regional emissions of scattering and absorbing aerosols also significantly affect both local and distant precipitation patterns (Westervelt et al., 2017, 2018). Considering the ambitious goals of the Paris Agreement, it is becoming increasingly essential to understand the impact of aerosols and other short-lived climate forcers on total anthropogenic radiative forcing (Lund et al., 2019).

Prolonged exposure to ambient PM<sub>2.5</sub> has been linked to various negative health effects, such as increased mortality from cardiovascular and cerebrovascular diseases, acute lower respiratory infections, lung cancer, and adverse birth outcomes (Burnett et al., 2018; Chowdhury et al., 2020, 2022; Cohen et al., 2017). The current human health effects of PM<sub>2.5</sub> are substantial with a more recent estimate of 8.1 million deaths per year (GBD, 2024). The future impacts of air pollutants will be influenced by both changes in emissions and shifts in demographics (Lund et al., 2019; Wells et al., 2024).

Africa exhibits distinct regional characteristics in aerosol emission sources, resulting in a wide range of potential future pollutant emission pathways, with some scenarios predicting significant increases in pollutants in key regions (Abera et al., 2020; Shindell et al., 2022; Turnock et al., 2020; Wells et al., 2024). Ongoing and anticipated future changes in Africa, including rapid economic development, rising urbanization, continued dependence on traditional biomass fuels, agricultural practices, limited access to advanced pollution control technologies, infrastructure expansion, and population growth, are expected to increase exposure to air pollutants (Abera et al., 2020; Bauer et al., 2019; Chowdhury et al., 2020; Wells et al., 2024). Despite this, research on air pollution-related health impacts in Africa, particularly outdoor air pollution, is limited (Abera et al., 2020; UNEP, 2022; Wells et al., 2024) due to the scarcity of observational data (Katoto et al., 2019).

Global emission inventories, including the Community Emissions Data System (CEDS) (Hoesly et al., 2018), the Evaluating the Climate and Air Quality Impacts of Short-Lived Pollutants (ECLIPSE) inventory from the Greenhouse Gas-Air Pollution Interactions and Synergies (GAINS) model (Amann et al., 2011), and the Emissions Database for Global Atmospheric Research (EDGAR) (Crippa et al., 2018; Janssens-Maenhout et al., 2019), as well as global emission scenarios such the Shared Socioeconomic Pathways (SSPs) (Riahi et al., 2017), have improved our understanding of emissions trends. However, Africa remains critically understudied due to limited data. This knowledge gap is particularly pressing given Africa's anticipated development and the wide range of emission sources across the region. Addressing this gap, our study focuses on African aerosol and precursor emissions, examining their climate and health impacts under



various scenarios. This work provides critical insights into Africa's unique emissions landscape and lays the groundwork for future research and policy interventions.

80

We explore the range in projections of mid-century anthropogenic air pollution levels in Africa, and the associated region-specific health impacts, resulting from 10 different pathways: SSP1-1.9, 2-4.5, 3-7.0, and 5-8.5 (Riahi et al., 2017); ECLIPSE Version 6b (ECL6) CLE, MFR, and SDS (IIASA, 2024); and the United Nations Environment Programme's (UNEP) Integrated Assessment of Air Pollution and Climate Change in Africa Baseline, Short-Lived Climate Pollutants (SLCP), and Agenda 2063 scenarios (UNEP, 2022) using the Oslo chemical transport model (OsloCTM3). We present estimates of the projected future regional radiative forcing of anthropogenic aerosols across these scenarios. We also evaluate the modelled PM<sub>2.5</sub> for 2019, driven by CEDS21 anthropogenic emissions, against surface observations and the modelled Aerosol Optical Depth (AOD) against the Moderate Resolution Imaging Spectroradiometer (MODIS) Level-3 atmosphere daily global AOD (550 nm). We build upon and expand on previous studies by incorporating simulations of PM<sub>2.5</sub>, its associated radiative forcing, and health impacts across a comprehensive range of scenarios, including SSPs, ECLIPSE, and UNEP pathways, to explore a broad spectrum of future possibilities under plausible conditions, and using a chemical transport model with a more detailed representation of the chemistry involved in formation of PM.

95

In Section 2, we provide an overview of the study domain and the OsloCTM3 model. We describe the emissions, simulations, observed and satellite data, and the methodologies for assessing health impacts and calculating radiative forcing. Section 3 discusses the results, highlighting the significant variability and regional heterogeneity in projected air pollution emissions across sub-Saharan Africa. We examine the sectoral contributions to BC and SO<sub>2</sub> emissions under increasing scenarios for 2020 and 2050, and the differences between these years. The section also discusses sub-regional and continental annual mean PM<sub>2.5</sub> changes between 2050 and 2015-2018 across all scenarios. Furthermore, we discuss the excess number of deaths attributable to PM<sub>2.5</sub> for 2015-2018 and 2050 under each scenario. In Section 4, we discuss the implications of our results, while Section 5 presents the conclusions and the key findings from the study and their broader implications.

100

105

## 2. Methods

110

### 2.1 Study Domain

115

In this study, we divided the African continent into five sub-regions: Western, Central, Eastern, Southern, and Northern, as illustrated in **Figure 1**. These regions were adapted from the WHO African regions (WHO, 2024), with minor adjustments to ensure comprehensive coverage of the entire continent. We examine the implications of projected mid-century anthropogenic air pollution levels across Africa, along with their associated health and climate impacts.

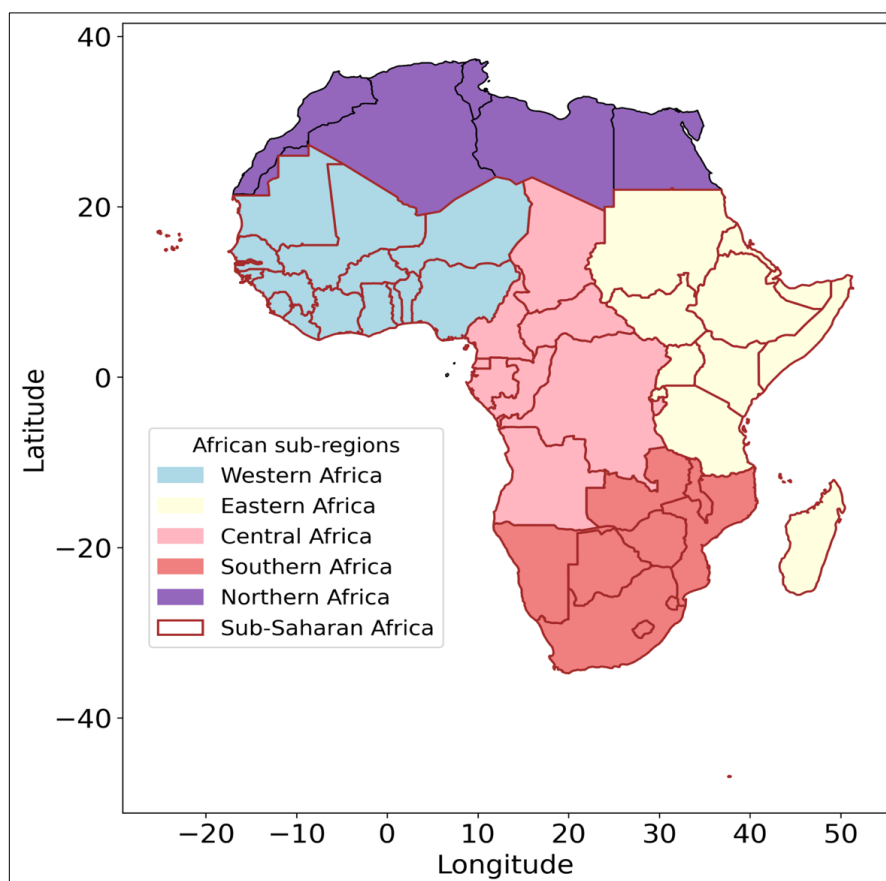


**Figure 1:** Study domain with regional definitions

## 2.2 Emissions

We use both baseline (2015-2018) emissions and projected emissions for the year 2050 from ten available pathways: SSP 1-1.9, 2-4.5, 3-7.0, and 5-8.5 (Riahi et al., 2017); ECL6 CLE, MFR, and SDS (IIASA, 2024); and UNEP Baseline, SLCP, and Agenda 2063 scenarios (UNEP, 2022). The ECL6 Version 6b covers the years 1990 - 2050 and includes gridded aerosol and reactive gas emissions at 5 and 10-year intervals. It also includes several other updates over earlier ECLIPSE versions, such as improved regional resolution, particularly for Africa, updates to legislation and historical data, and revised gridding patterns for various sectors, including power plants, flaring, transportation, and industry (IIASA, 2024). We used 2016 ECL6 emissions as the baseline for calculating future changes in ECLIPSE.

Gidden et al. (2019) provides gridded SSP air pollution emissions from 2015 to 2100 across sectors, including residential, industrial, energy, transportation, waste, agriculture, solvents, and international shipping. SSP1-1.9 represents a scenario with rigorous air pollution



135 control, low climate forcing, and minimal challenges in mitigation and adaptation, while SSP3-7.0  
is marked by weak air pollution control, high climate forcing, and significant challenges in both  
mitigation and adaptation (Riahi et al., 2017). SSP2-4.5 serves as an intermediate pathway, while  
SSP5-8.5 is characterized by high socio-economic challenges for mitigation and low socio-  
economic challenges for adaptation (O'Neill et al., 2017).

140

A recent UNEP report provides a comprehensive assessment of the interactions between  
air pollution and climate change in Africa (UNEP, 2022), bringing a unique focus on emissions  
scenarios specifically to Africa for the first time. This assessment utilizes the Low Emissions  
Analysis Platform (LEAP) system, a prominent software tool for integrated energy policy planning,  
145 emissions reduction, and climate change mitigation evaluations (LEAP, 2021). We used the three  
UNEP scenarios: Baseline, SLCP, and Agenda 2063 for 2018 and 2050. The Baseline scenario  
assumes that the energy, agricultural, and waste sectors will continue their current paths and that  
no new policies will be developed, in contrast, the SLCP scenario calls for the implementation of  
mitigation measures that specifically target the main sources of SLCPs, such as BC (UNEP,  
150 2022). Most of the actions in this scenario are of a technological nature, like advances in  
technology and fuels. The Agenda 2063 scenario is a more ambitious scenario, which  
concentrates on mitigating measures that more widely accomplish the objectives of the  
Sustainable Development Goals (SDGs) and the African Union Commission (AUC) Agenda 2063  
(UNEP, 2022). This scenario begins with the SLCP measures from the previous scenario and  
155 then adds both technical and behavioral mitigating mechanisms that lead to greater  
transformative change.

Since the UNEP emissions are provided only for the African domain, we used SSP2-4.5  
emissions for the rest of the world. As part of this we also merged UNEP sector categories to  
160 align with those in the SSPs. Specifically, this means UNEP sectors residential, services,  
agricultural energy, and unspecified categories were merged into one residential category,  
industry and industrial processes into industry, electricity, oil and gas, and charcoal into energy,  
and livestock and crop production into agriculture. Transport and waste are provided as individual  
categories in both SSPs and UNEP scenarios. International shipping is not provided by UNEP,  
165 and we therefore used SSP2-4.5 emissions.

### 2.3 OsloCTM3

The OsloCTM3 is a global, three-dimensional Chemical Transport Model (CTM), driven  
by three-hourly meteorological forecast data from the European Centre for Medium-Range  
170 Weather Forecasts (ECMWF) Open Integrated Forecast System (OpenIFS) (Lund et al., 2018,  
2019; Søvde et al., 2012). These forecasts are generated daily, starting with a 12-hour spin-up  
period beginning from a noon analysis of the previous day, which are then combined to create a  
uniform dataset for an entire year (Søvde et al., 2012). The model is run in a  $2.25^\circ \times$   
 $2.25^\circ$  horizontal resolution and includes 60 vertical levels, with the highest level centered at 0.1  
175 hPa. OsloCTM3 simulates atmospheric concentrations of trace gases and all the main climate  
relevant aerosol species (black carbon, primary and secondary organic aerosol, secondary  
inorganic aerosol, sea salt and dust). The model description and evaluation of simulated aerosol  
distributions have been recently documented in Lund et al. (2018, 2019).

180 For each case, the model is run for 18 months, discarding the first 6 as spin-up.  
Meteorological data from the year 2010 OpenIFS were used for all simulations of the baseline  
and future, with no feedback from climate change or variations in natural aerosols. This allows us



185 to isolate the impact of anthropogenic emissions on air quality from the impacts of future climate changes on aerosols and trace gases. We performed simulations using the ECLIPSE and UNEP emissions. We use data from experiments with SSP1-1.9, SSP2-4.5, and SSP3-7.0 emissions performed for Lund et al. (2019) and perform an additional simulation using SSP5-8.5 emissions for this study.

190 Results from simulations with future (2050) emissions are compared to simulations with the corresponding baseline emissions. The available emission scenarios have somewhat different baseline (i.e. most recent historical) years: 2015 for the SSPs, 2016 for ECL6 emissions, and 2018 for UNEP emissions. The difference in simulated  $PM_{2.5}$  concentrations between these three base years is 2 % on a continent-wide annual average (**Figure S3**), suggesting limited influence on our analysis from the differing time period considered. We also perform an evaluation of  
195 OsloCTM3 performance against observations over Africa (see Sect. 2.4). For this we use additional data from simulations with the CEDS21 emissions as input, to capture the most recent global emission inventory. These simulations were performed for and documented in Lund et al. (2023), however, neither model validation nor a dedicated Africa-focus was part of that study.  $PM_{2.5}$  was calculated as the sum of individual fine-mode aerosol species, namely BC, primary and secondary organic aerosol (POA, SOA), sulfate ( $SO_4$ ), dust, sea salt, nitrate ( $NO_3$ ), ammonium ( $NH_4$ ).

200 We analyzed the differences in population weighted  $PM_{2.5}$  between future emissions and 2015, 2016, or 2018 depending on the scenario as described above. Annual global population data at a  $0.5^\circ$  resolution was obtained from the Inter-Sectoral Impact Model Intercomparison Project (ISIMIP2b) simulations (Jones and O'Neill, 2016). Both the OsloCTM3  $PM_{2.5}$  data and the population data were regridded to a  $1^\circ$  latitude by  $1^\circ$  longitude resolution using bilinear interpolation prior to calculating population-weighted values. Since the model can also be run in this resolution, the downscaling provides sufficient spatial resolution to capture major spatial  
210 variations in both  $PM_{2.5}$  concentrations and population distributions. These values were computed on a country-by-country basis by summing the products of population and  $PM_{2.5}$  concentration at the grid level within each country and then dividing by the total population of that country (Chowdhury et al., 2019; Southerland et al., 2022). SSP2 population data was used for UNEP and ECLIPSE cases, while the respective SSPs population projections were matched for the other  
215 SSP scenarios.

Using offline radiative transfer calculations with a multi-stream model using the discrete ordinate method (Myhre et al., 2013; Stamnes et al., 1988), we derived the AOD and the instantaneous top-of-the-atmosphere radiative forcing due to aerosol–radiation interactions  
220 resulting from changes in anthropogenic emissions. We also include an estimate of the radiative forcing of aerosol–cloud interactions using a parameterization of based on Quaas et al. (2006) to account for the change in cloud droplet concentration resulting from anthropogenic aerosols, which alter the cloud effective radius and thus the optical properties of the clouds. The method has been used in several previous studies (e.g. (Lund et al., 2019, 2023; Myhre et al., 2013, 2017)). Note that this method excludes any contributions from cloud lifetime changes, which are  
225 typically estimated to be smaller than cloud albedo effects but not negligible (Stjern et al., 2016).

## 2.4 Observations

We evaluated the OsloCTM3, driven by CEDS21 anthropogenic emissions, against  $PM_{2.5}$  surface observations from various United States embassy locations in Africa for the year 2019,



as a first-order sanity check. The observed data was obtained from the AirNow database (U.S. EPA, 2024). Additionally, we compared the model's  $PM_{2.5}$  estimates with high-resolution satellite-derived  $PM_{2.5}$  estimates, which were obtained from combined AOD retrievals from National Aeronautics and Space Administration (NASA) MODIS, Multi-angle Imaging Spectroradiometer (MISR), and Sea-viewing Wide Field-of-view Sensor (SeaWiFS) instruments, integrated with the Goddard Earth Observing System Chemistry (GEOS-Chem) transport model. These data are available in the Satellite-derived  $PM_{2.5}$  Archive (Van Donkelaar et al., 2021). The model's performance was assessed using the coefficient of determination ( $R^2$ ), root mean squared error (RMSE) and mean absolute error (MAE).

We evaluated the modelled AOD from CEDS21 against data retrieved from the MODIS instrument aboard the Aqua satellite, specifically the MYD08\_D3\_V6.1 release, which was accessed via the NASA Giovanni interface for the year 2019. The MYD08\_D3 product is a level-3 gridded daily global dataset from MODIS (Platnick, 2015). It provides daily averaged values for atmospheric parameters on a  $1^\circ \times 1^\circ$  grid, including aerosol properties, total ozone, atmospheric water vapor, cloud characteristics, and atmospheric stability indices (Platnick, 2015). For our analysis, we used the combined Dark Target and Deep Blue AOD at 550 nm from this release.

## 2.5 Health impact assessment

In combination with the generated data on ambient  $PM_{2.5}$  exposure, we apply the MR-BRT (meta-regression-Bayesian, regularized, trimmed) exposure-response function (Murray et al., 2020; Pozzer et al., 2023), which was also used in our previous studies (Chowdhury et al., 2022, 2024) and the most recent iteration of the Global Burden of Disease study. Using the cause-specific exposure-response function, we estimate excess deaths from ischemic heart disease (IHD), stroke (both ischemic and hemorrhagic), chronic obstructive pulmonary disease (COPD), lung cancer (LC), and Type II diabetes (T2DM) among adults (aged 25 and above), as well as acute lower respiratory tract infections (ALRI) among children (under 5 years old). The excess death burden was calculated at a  $25 \times 25$  km spatial resolution by interpolating the modeled ambient concentration data, and the estimates were stratified by age and disease category, following the approach of our previous studies:

$$M_{c,a,d} = P_a \times BM_{a,d} \times \frac{RR_{c,a,d} - 1}{RR_{c,a,d}} \quad (\text{Eq. 1})$$

Excess deaths were estimated separately for adults and children at each 5-year interval.  $RR_{c,a,d}$  were derived using MR-BRT functions for all diseases by age, where c,a,d denotes concentration of  $PM_{2.5}$ , population age and disease respectively. Age specific RRs (Relative Risks) for IHD and stroke, are obtained using MR-BRT. For LC, T2-DM, and COPD uniform  $RR_{c,d}$  were used across all age groups among adults.  $BM_{a,d}$  is the baseline mortality rate per 100,000 population, obtained from the GBD (GBD, 2024) for all countries in Africa for the years 2015, 2016 and 2018. For 2050, we use the projected baseline under SSP scenarios mortality rates generated in a previous study by combining information from GBD and International Futures (Yang et al., 2023). We considered BM to remain uniform within a country at  $25 \times 25$  km resolution by age and disease.  $P_a$  is the exposed population in a grid by age; the age distributions at 5-year intervals (adults  $> 25$  years), and  $< 5$  years for children were obtained from the SSP database (Riahi et al., 2017) which are then merged with the gridded population data at about  $25 \times 25$  km<sup>2</sup> horizontal resolution under the respective SSP scenarios to obtain the age-specific population



( $P_a$ ) at each  $5 \times 5 \text{ km}^2$  grid. For the concentration data generated using SSP emissions, we apply the respective SSP projections for baseline mortality and population. For other emission scenarios (UNEP and ECL6), we utilize the SSP2 projections, as they align closely with the UN population data.

## 3. Results

### 3.1 Projected air pollution emission trends

There is a large spread and regional heterogeneity in projected air pollution emissions across sub-Saharan Africa and its sub-regions (**Figure 2 and Figure S4**). This variability suggests that the differences in local regulations, technological advancements, and economic development trajectories can substantially influence emission trends. As such, regional policy differences may play a crucial role in reducing uncertainties in emissions projections. While we focus on the year 2050, we here show the full UNEP and SSP timeseries to illustrate that the spread in emissions continues through the century. We note that there are other scenarios in the ECL6 and SSP databases, but the ones considered in the present study span the large range shown in **Figure 2**.

BC emissions in sub-Saharan Africa are projected to increase under SSP370, SSP585, SSP245, UNEP Baseline, and ECL6 CLE by 2050, while they are projected to decrease under SSP119, UNEP SLCP, UNEP 2063, ECL6 MFR, and ECL6 SDS scenarios. Notably, there are projected declines in BC emissions after mid-century under SSP245 and SSP245. The largest increases in BC emissions are projected under the UNEP Baseline and SSP370 scenarios, with increases of 1,937 kt/year (110 %) and 961 kt/year (45 %), respectively. In contrast, the largest declines in BC emissions are projected under the ECL6 SDS and SSP119 scenarios, with reductions of 1,956 kt/year (94 %) and 1,793 kt/year (84 %), respectively (**Table S2**). After mid-century, BC emissions in sub-Saharan Africa are projected to decline under the SSP585 scenario, likely driven by a reduction in residential fossil fuel use (Wells et al., 2024). Similarly,  $\text{SO}_2$  emissions in sub-Saharan Africa are projected to decline under both SSP585 and SSP119, likely driven by reductions in industrial fossil fuel use. BC emissions in sub-Saharan Africa under the SSP119 scenario are projected to fall rapidly to around 25 % of their present-day levels by 2050, whereas under the SSP370 scenario, BC emissions are projected to be the largest globally by 2100, surpassing East Asia (Lund et al., 2019). Organic carbon (OC) and nitrogen oxides ( $\text{NO}_x$ ) exhibit similar trends (**Figure S4**); however, OC decreases under the SSP585 scenario.

For  $\text{SO}_2$  emissions, the overall pattern in sub-Saharan Africa shows projected increases under all scenarios by 2050 except for ECL6 CLE, ECL6 MFR, and ECL6 SDS, with declines after mid-century under SSP119, SSP245, and SSP585. The largest increases in  $\text{SO}_2$  emissions are projected under the UNEP baseline and UNEP SLCP scenarios, with increases of 8,675 kt/year (144 %) and 7,591 kt/year (125 %), respectively, while the largest decreases are projected under the ECL6 SDS and ECL6 MFR scenarios, with reductions of 7,920 kt/year (86 %) and 5,505 kt/year (60 %), respectively. BC emissions decline under the UNEP SLCP scenario by 2050, however,  $\text{SO}_2$  emissions increase dramatically under UNEP SLCP by 2050 as this is a scenario focusing on reducing short-lived climate pollutants with an overall climate warming effect, such as BC emissions from residential, transport, agriculture, and waste sectors, methane emissions from agriculture, waste, and fossil fuel emissions from industrial processes—without addressing  $\text{SO}_2$  emissions. The UNEP SLCP scenario envisions a transition where 90 % of wood and charcoal use switches to efficient stoves by 2063 in urban areas, with similar shifts in rural areas. It also assumes a gradual transition from gas and liquefied petroleum gas (LPG) to efficient



electricity starting in 2030 (UNEP, 2022). The UNEP Agenda 2063 scenario shows a decline in both BC and SO<sub>2</sub> emissions by 2050. This scenario assumes a 1.4 % annual decrease in energy intensity for household energy use (compared to constant levels in the baseline), a 93 % improvement in refrigerator efficiency by 2063, and a doubling of air conditioner efficiency (UNEP, 2022). Additionally, it assumes that 30 % of passenger kilometers shift from cars to buses, and 25 % switch to cycling.

Additionally, BC, SO<sub>2</sub>, OC, and NO<sub>x</sub> emissions in the sub-regions are projected to follow similar trends to those in sub-Saharan Africa; however, certain regions are projected to maintain high SO<sub>2</sub> emissions even under some stringent scenarios. For instance, Central Africa and Southern Africa SO<sub>2</sub> emissions are projected to increase substantially by 2050 under the SSP119 scenario, with increases of 4,240 kt/year (303 %) and 3,138 kt/year (47 %), respectively, driven by reliance on coal during the transition period. Under the SSP585 scenario, SO<sub>2</sub> emissions are projected to increase substantially in Western Africa and Eastern Africa, with projected increases of 2,208 kt/year (429 %) and 2,561 kt/year (402 %), respectively, by 2050, driven by energy and industrial emissions (Shindell et al., 2022; Wells et al., 2024). Northern Africa BC and SO<sub>2</sub> emissions are projected to increase substantially under the SSP370, by 2050. The increases in sub-regional BC, SO<sub>2</sub>, OC, and NO<sub>x</sub> emissions are projected to decline after mid-century under most SSP scenarios, with the exception of SSP370, where an increase is projected in some regions, while certain regions may still see a decrease. Under the UNEP baseline scenario, BC, OC, NO<sub>x</sub> emissions are projected to be largest in Western Africa and Eastern, followed by Central Africa, Southern Africa, and Northern Africa, by 2050, while SO<sub>2</sub> emissions are projected to be largest in Southern Africa, followed by Eastern Africa, Northern Africa, Western Africa, and Central Africa (**Table S2**).

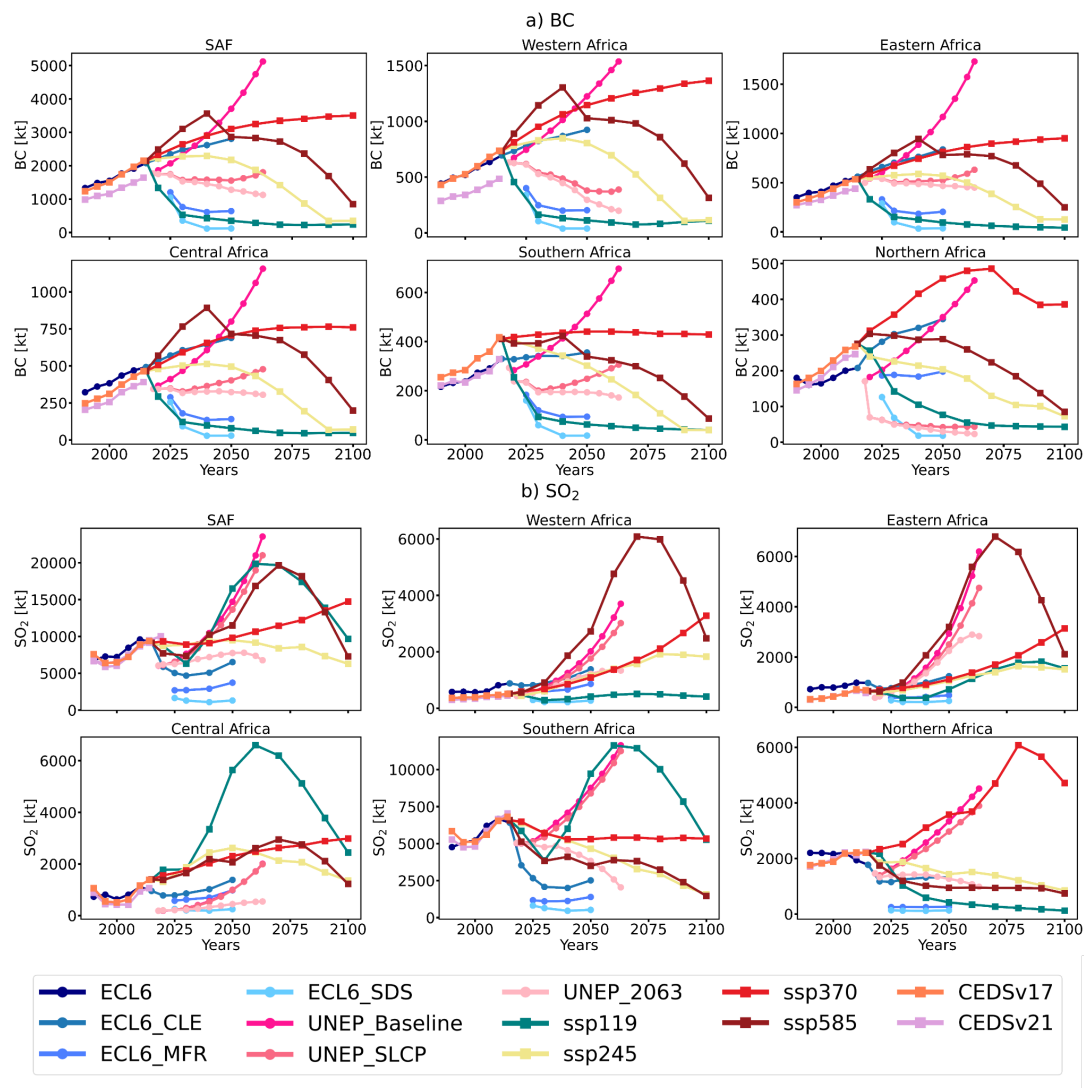


**Figure 2:** Large spread and regional heterogeneity in projected air pollution emissions in sub-Saharan Africa. Here shown for a) BC and b) SO<sub>2</sub>.

**3.2 Sectoral contributions to air pollution emissions**

In many cases, the emissions source distributions are distinct, with notable discrepancies in sectoral shares across regions, as exemplified in **Figures 3 and 4** for the increasing scenarios SSP370, ECL6 CLE and UNEP Baseline emissions in 2020 and 2050. For instance, in Eastern Africa, the UNEP baseline scenario attributes 58 % of 2020 BC emissions to the residential sector, while the ECL6 CLE scenario attributes 75 %, and SSP370 attributes 84 %. Different socio-economic projections, technological advancements, and policies influence the regional emission



360 sources and sectoral contributions. Consequently, the discrepancies in sectoral emission  
distributions among UNEP, SSPs, and ECL6 highlights the need for accurate activity data and  
harmonization, particularly in the upcoming 7th Assessment Report of the Intergovernmental  
Panel on Climate Change (IPCC AR7).

365 The residential sector is the largest contributor to BC emissions across sub-Saharan Africa  
in all increasing scenarios in 2020 and 2050. In Northern Africa, BC emissions are dominated by  
the transportation sector across all increasing scenarios. The widespread use of clean cooking  
fuels, such as natural gas and Liquefied Petroleum Gas (LPG), by the majority of the population  
370 in Northern Africa (IEA, 2020) explains the comparatively lower residential emissions in this sub-  
region. Under SSP370, the residential sector will contribute 86 % in Western Africa, 84 % in  
Central Africa, 83 % in Eastern Africa, and 75 % in Southern Africa. The shipping emissions  
increases are unique to SSP3-7.0. The second-largest contributor to BC emissions change under  
SSP370 is international shipping (5-12 %) across the various regions. These emissions from  
international shipping cannot be attributed to African nations but may be linked to increasing trade  
375 associated with economic development. In Northern Africa, the transportation sector will  
contribute 61 % of the total BC increase under this scenario, followed by international shipping at  
12 %. Additionally, under the SSP585, Western Africa and Eastern Africa show an increase in  
the share of BC emissions from the energy sector, which is not evident in Central Africa (**Figure  
S5 and S6**), suggesting more influence from energy generation as Western Africa and Eastern  
Africa further electrify. However, in Southern Africa and Northern Africa, BC emissions are  
380 projected to decrease under SSP585 by 2050, with the residential sector and transportation sector  
being the largest contributors to these reductions, respectively

By 2050, under the ECL6 CLE scenario, the transportation and waste sectors will be the  
second and third largest contributors to BC emissions in sub-Saharan Africa, following the  
residential sector. There will be a reduction in the residential sector's contribution to total BC  
385 emissions and an increase in the contributions from the transportation and waste sectors. For  
instance, in Western Africa, 77 % and 8 % of BC emissions are projected to come from the  
residential sector and transportation sector by 2050, compared to 83 % and 5 % respectively, in  
2020. The sectoral contributions to emissions changes (increases or decreases) in UNEP  
Baseline stand in sharp contrast with the SSPs which are mainly dominated by changes in  
390 household biomass cooking. For instance, in Western Africa, the transportation and residential  
sectors will account for 52 % and 27 % of the increase, respectively, in contrast with SSPs which  
were mostly dominated by residential emission changes alone.

Similarly, the major sectoral contributors to SO<sub>2</sub> emissions in each sub-region of Africa are  
the industrial, energy, and transportation sectors, depending on the scenario (**Figure 4, Figure  
395 S7 and S8**). The SSPs indicate a shift in Africa's industrial center away from South Africa, as it  
stands at present, and more towards other further north regions of Africa as they grow and  
industrialize. The SSPs also demonstrates the impact of assumptions used to generate air  
pollution scenarios, depending on economic status of the region or countries, the air quality  
policies are assumed to be implemented on different time scales (Rao et al., 2017). By 2050,  
400 under SSP370, SO<sub>2</sub> emissions are projected to increase substantially in Western, Central,  
Eastern, and Northern Africa, with industrial sectors contributing 49 % in Western Africa, 86 % in  
Central Africa, 49 % in Eastern Africa, and 44 % in Northern Africa, which hints at a rapid  
industrialization and sweeping changes in economic activity. In contrast, Southern Africa's SO<sub>2</sub>  
emissions are projected to decrease under SSP370, with the industrial sector contributing 64 %



405 and the energy sector contributing 27 % to this reduction. The energy sector's contribution to  
total SO<sub>2</sub> emissions in sub-Saharan Africa under the SSPs is projected to decrease, while the  
industrial sector's contribution is projected to increase (**Figure S7 and S8**). Additionally, Under  
the ECL6 CLE scenario, by 2050, the industrial sector and the energy sector are projected to be  
410 the dominant contributors to the increase in SO<sub>2</sub> emissions in sub-Saharan Africa, except in  
Southern Africa, where SO<sub>2</sub> emissions are projected to decrease, with the industrial sector  
accounting for 56 % of this reduction.

Unlike the SSP counterparts, the UNEP Baseline scenario suggests a more distributed  
emissions profile across African sub-regions in 2050, similar to ECL6, particularly with regard to  
415 transportation emissions, which are more muted in the SSPs. Furthermore, Under the UNEP  
Baseline scenario, the largest sectoral contributors to emissions are projected to be the transport,  
energy, and industrial sectors in Western Africa, Central Africa, Eastern Africa, and Northern  
Africa, while in Southern Africa, the energy and residential sectors are projected to be the largest  
contributors. Additionally, reductions in agricultural waste burning on fields in sub-Saharan Africa  
420 by 2050 are projected under the UNEP Baseline scenario, as well as the SSPs and ECL6, due to  
the adoption of alternative agricultural practices, improved waste management, and emissions-  
reducing technologies.

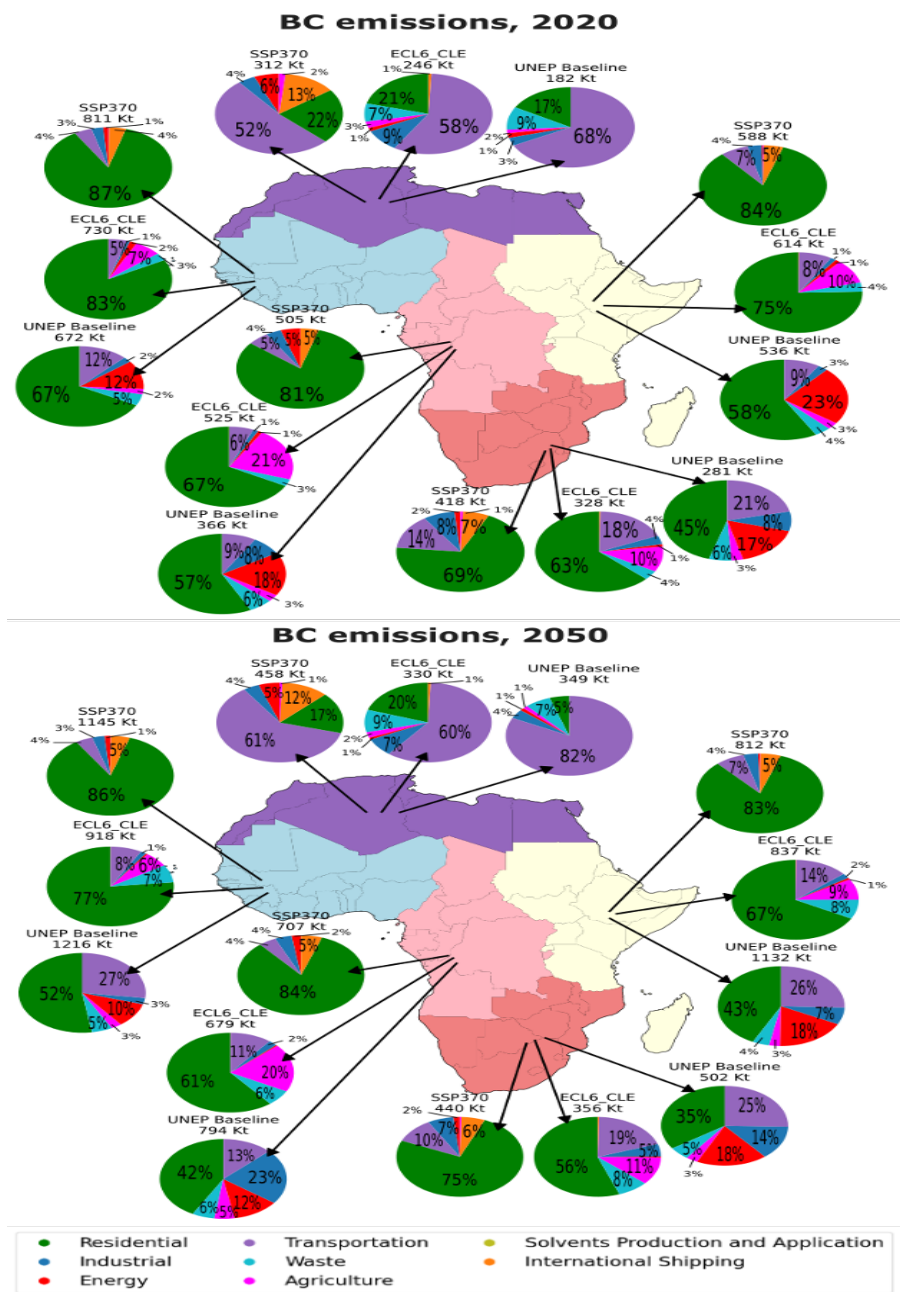


**Figure 3:** Sub-regional sectoral contributions to BC emissions (kilotons per year) in increasing scenarios for 2020 and 2050

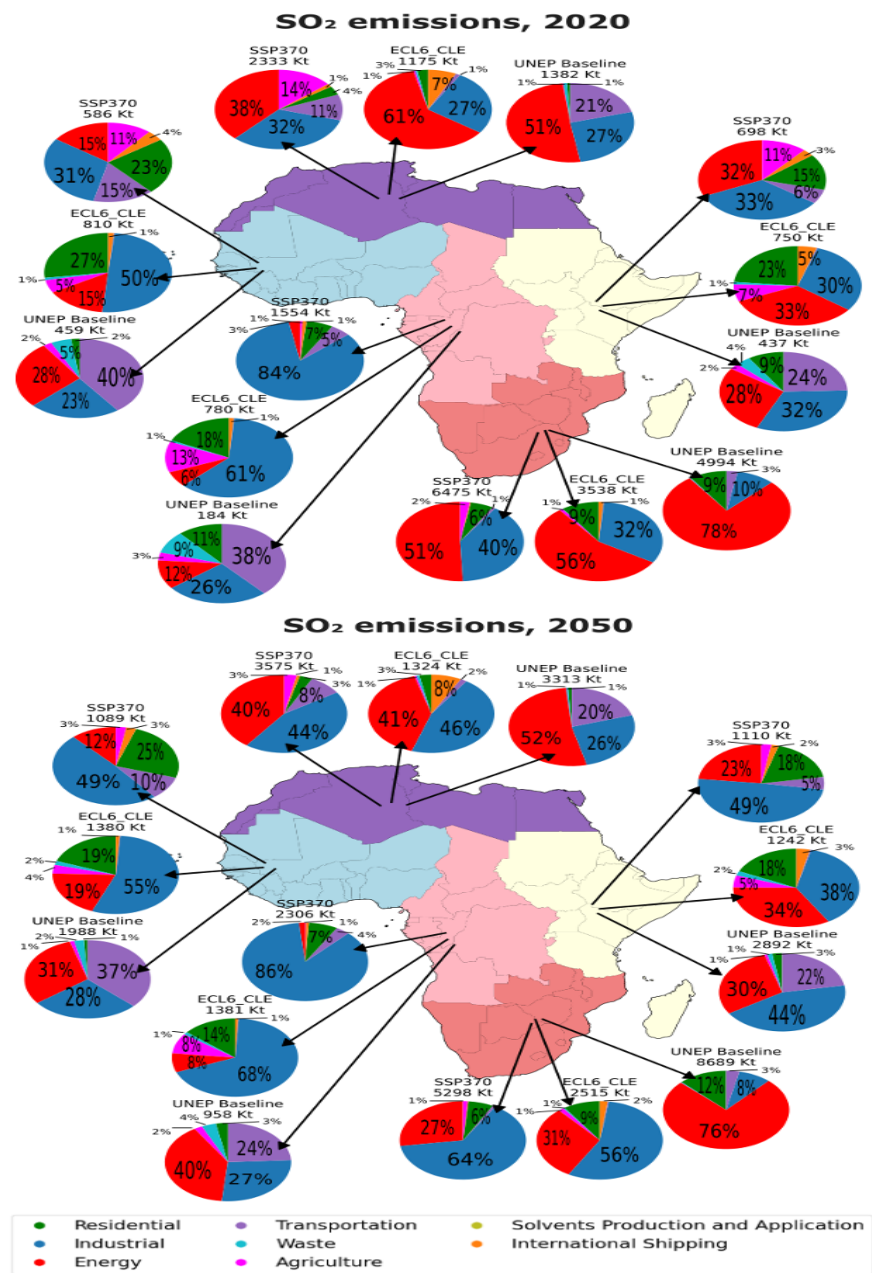


**Figure 4:** Sub-regional sectoral contributions to SO<sub>2</sub> emissions (kilotons per year) in increasing scenarios for 2020 and 2050



### 3.3 Annual-mean population-weighted PM<sub>2.5</sub> concentrations

The OsloCTM3 model has been validated against PM<sub>2.5</sub> surface observations for 2019 and MODIS Aqua AOD data across Africa, providing a broad range of performance upon validation. For PM<sub>2.5</sub> surface observations, R<sup>2</sup> values range from 0.48 to 0.76, and MAE values range from 5.7 µg m<sup>-3</sup> to 23.8 µg m<sup>-3</sup> in Western and Central Africa. For MODIS Aqua AOD, the validation yields an R<sup>2</sup> of 0.36, with RMSE and MAE of 0.11 and 0.08, respectively (see **Figure S1**, **Figure S2**, and **Table S1** for details). Overall, these validation results indicate that OsloCTM3 captures key spatial and temporal variations in PM<sub>2.5</sub> and AOD across Africa, though with varying performance across regions.

Given the model's reasonable performance for present-day, we now examine projected changes in future PM<sub>2.5</sub> levels. We examined the difference in annual-mean PM<sub>2.5</sub> concentrations between the highest scenario (UNEP Baseline) and the lowest scenario (SSP119) for sub-Saharan Africa as a whole in 2050. Surface PM<sub>2.5</sub> concentrations differ by up to a factor of 2 between the highest and lowest scenario when averaged across the African continent in 2050, with markedly higher local spread (**Figure 5**). Notably, the most substantial differences between the UNEP Baseline and SSP119 are observed in Nigeria, Benin, Niger, Uganda, Ethiopia, Kenya, Democratic Republic of the Congo, and Egypt, where PM<sub>2.5</sub> concentrations differ by as much as 20 µg m<sup>-3</sup> (75 %) in 2050 projected populations. Most of these regions, which are characterized by high population density and industrial activity, experience elevated pollution in the UNEP scenario, highlighting the need for aggressive emission reduction measures.

Furthermore, regionally-averaged annual-mean population weighted (P.W.) PM<sub>2.5</sub> concentrations are projected to increase under UNEP Baseline, SSP370, and ECL6 CLE scenarios, and decrease under the other scenarios, by 2050 when averaged across the African continent (**Figure 6**). The largest increase is projected under the UNEP Baseline scenario, with an increase by up to 6 µg m<sup>-3</sup> (37 %) in Eastern Africa, while the largest decrease is projected under the ECL6 SDS scenario, with a reduction by up to 5 µg m<sup>-3</sup> (8 %) in Western Africa and 3 µg m<sup>-3</sup> (39 %) in Southern Africa. Projected annual PM<sub>2.5</sub> concentrations in sub-Saharan Africa follow a similar trend, with an increase of 4 µg m<sup>-3</sup> (16 %) under the UNEP Baseline scenario and a decrease of 5 µg m<sup>-3</sup> (22 %) under the ECL6 SDS scenario. Western, Eastern, and Northern Africa are projected to experience the most substantial PM<sub>2.5</sub> exposure levels under the UNEP Baseline, SSP370, and ECL6 CLE scenarios due to increased emissions from residential, industrial, transportation, and energy sectors. Conversely, the most substantial decreases are projected under the ECL6 SDS, ECL6 MFR, and SSP119 scenarios (**Figure 6** and **Table S2**).

In Southern Africa, annual PM<sub>2.5</sub> levels are projected to decrease under the SSP370 and ECL6 CLE scenarios by 0.6 µg m<sup>-3</sup> (6 %) and 0.3 µg m<sup>-3</sup> (3 %), respectively, primarily due to reductions in energy and industrial emissions. However, Western and Eastern Africa show slight increases under the SSP245 scenario (1 %) and UNEP SLCP scenario (7 %), respectively. The most substantial increases in PM<sub>2.5</sub> exposure are projected in Nigeria, Egypt, Uganda, Rwanda, Burundi, and Benin under the UNEP Baseline and SSP370 scenarios, with concentration increases ranging from 10 µg m<sup>-3</sup> to 20 µg m<sup>-3</sup> (11 % to 33 %) (**Figure S12**). Conversely, the largest decreases are observed in Nigeria under the ECL6 SDS, SSP119, and UNEP 2063 scenarios, followed by significant reductions in Uganda, Rwanda, Burundi, and Egypt. These observed differences largely reflect variations in PM<sub>2.5</sub> concentrations as well as shifts in population distribution.



In some areas the relative changes in  $PM_{2.5}$  concentrations are small despite notable absolute changes, which is attributed to naturally high baseline concentrations from sources like dust, which cause air quality limits to already be exceeded (Pai et al., 2022). The varying outcomes across scenarios emphasize the critical role of policy choices in determining future air quality in Africa. The benefits in Nigeria, Uganda, Rwanda, Burundi, and Benin will primarily result from improvements in the residential sector, which plays a dominant role in reducing BC emissions. In countries such as South Africa, the benefits will largely stem from reductions in industrial and energy sector emissions of  $SO_2$ . In Northern Africa, the benefits will be driven primarily by reductions in emissions from the transportation sector.

Generally, the results are consistent with the emissions changes (**Figs. 2-4**), in that stringent energy and air quality policy scenarios such as SDS, SSP119, MFR, and UNEP2063 result in PM decreases across the board, and more extractive and fossil-fuel dominated scenarios (UNEP BASE, SSP370, and CLE) result in worse future PM air quality. These results highlight the potential for effective policy interventions to mitigate air pollution and improve public health across the continent.

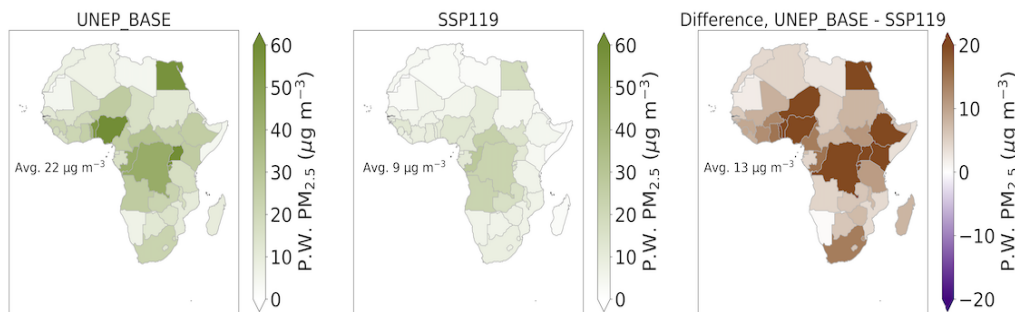


**Figure 5:** Annual-mean population-weighted  $PM_{2.5}$  concentrations in 2050 under the highest scenario (UNEP Baseline) and the lowest scenario (SSP119) for sub-Saharan Africa as a whole, along with their difference

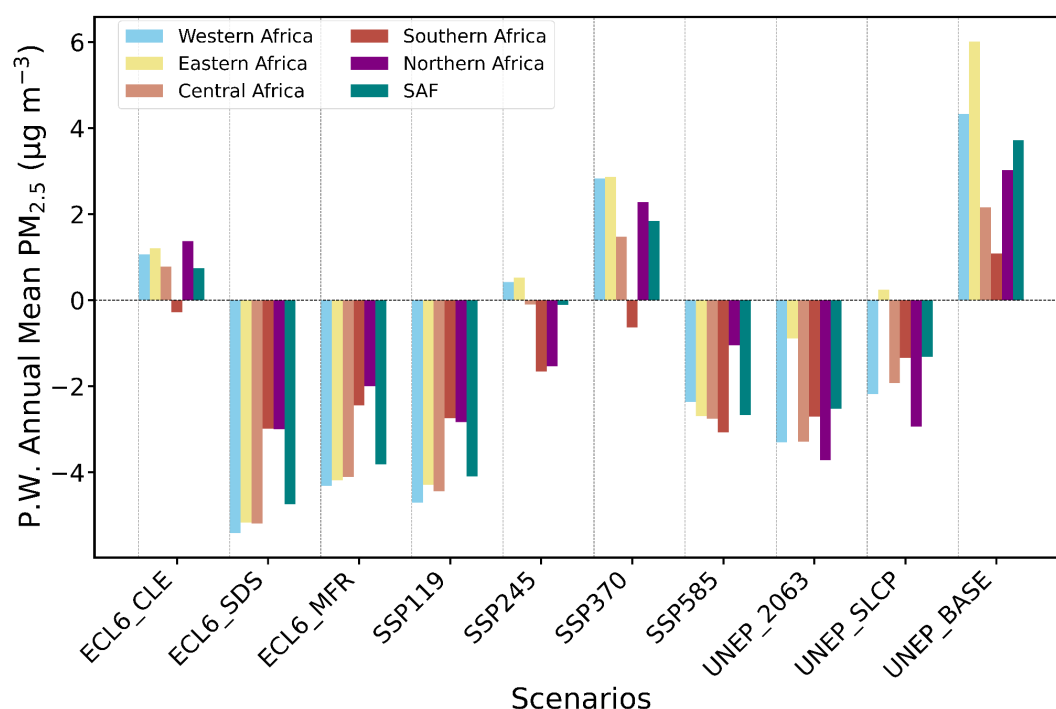


**Figure 6:** Regionally-averaged annual-mean population-weighted PM<sub>2.5</sub> concentrations in 2050 compared to the baseline.

### 3.4 Excess Deaths Attributable to PM<sub>2.5</sub>

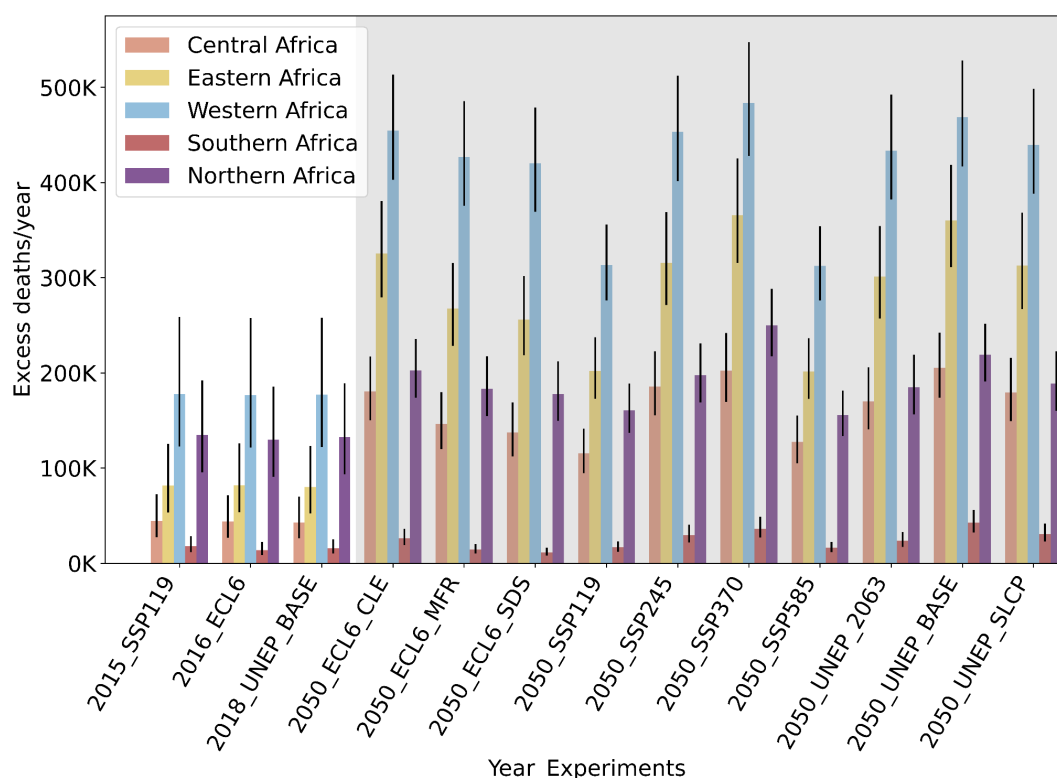
Building on the exposure results, we estimated the projected excess deaths per year due to PM<sub>2.5</sub> for baseline and 2050 emissions for each scenario. There are large increases in almost all cases partially due to the projected population increase (**Figure S13**). Africa's population is expected to double by 2050 growing from 1.1 billion to 2.3 billion, with Western African population reaching 0.9 billion, followed by Eastern Africa with 0.7 billion, Southern Africa with 0.26 billion, Central Africa with 0.24 billion, and Northern Africa with 0.22 billion (**Figure S11**). Western Africa is projected to have the largest excess deaths per year from ambient PM<sub>2.5</sub> across all scenarios, followed by Eastern Africa, Northern Africa, Central Africa, and Southern Africa. By 2050, excess deaths in Western Africa are projected to increase by more than 2.5 times under the highest emissions SSP370 and UNEP Baseline scenarios, compared to 0.18 (95 CI: 0.12-0.24) million in the baseline period. Even under the lower emission SSP119 scenario, excess deaths are projected to increase by more than 1.5 times, driven by significant population growth (**Figure S11**). Southern Africa consistently has the lowest projected excess deaths per year across all scenarios, with estimates remaining under 0.05 million by 2050, although this represents up to a twofold increase compared to the baseline. The wide range across emission regions for the future is evident in the projected excess death estimates for all African regions, with projected



525 excess deaths varying by a factor of 1.8 times in Eastern and Central Africa, 1.5 times in Western Africa, and up to 2.6 times in Southern Africa.

Due to large increases in population size in all African regions,  $PM_{2.5}$ -attributed mortality is projected to increase in all scenarios between the baseline and near future, even in scenarios projecting modest  $PM_{2.5}$  decreases (ECL6 SDS, SSP1-1.9, UNEP 2063, etc) and strong decreases in baseline disease rates (depicted by prevalent negative blue bars for epidemiological transitions in **Figure S13**). This further highlight that there are already high  $PM_{2.5}$  concentrations due to fires and natural dust (Pai et al., 2022).

530



535 **Figure 7:** Excess deaths due to  $PM_{2.5}$  calculated for baseline and 2050 emissions for each scenario. The black bars represent error bars, showing the 95% confidence interval in the excess death estimates for each region and scenario.

### 3.5 Anthropogenic aerosol-inducing radiative forcing

540

In **Figure 8**, we show the net radiative forcing due to changes in anthropogenic aerosol emissions between 2050 and 2015, 2016 or 2018, depending on the emission scenario. This includes the radiative forcing due to aerosol-radiation interactions (RF<sub>ari</sub>, shown in **Figure S15**) and from aerosol-cloud interactions (RF<sub>aci</sub>, shown in **Figure S16**). Averaged over the entire continent, the RF<sub>ari</sub> in 2050 relative to the baseline is negative in the UNEP scenarios, SSP119,

545



and ECL6 SDS scenarios, and positive in the remaining scenarios, reflecting a small cooling or warming effect depending on the scenario. The RF<sub>aci</sub> is negative in the UNEP Baseline and UNEP SLCP and positive in the SSPs, UNEP Agenda 2063, and ECL6 scenarios.

550        A net positive aerosol forcing in 2050 relative to the baseline is projected in all but two scenarios, with regional-mean values ranging from 0.03 W m<sup>-2</sup> in SSP119 to 0.27 W m<sup>-2</sup> in SSP585. Regional patterns of aerosol forcing reveal negative and positive values in certain areas, depending on the scenario, and align closely with AOD changes (**Figure S14**). This shows the dominating influence of changes in scattering aerosols in the scenarios. Although local emission changes play the most important role, there could be influences from emission changes in surrounding regions via long-range transport. Southern Africa experiences anthropogenic aerosol-induced warming in all scenarios except UNEP BASE and UNEP SLCP. This warming reflects stricter policies and subsequent stronger emissions reductions (**Figure 2**). Since emissions of changes in scattering aerosols dominate, the result is a positive radiative forcing.

555

560        The regional pattern of radiative forcing reflects not only the overall stringency of air pollution control in the scenarios but also subsequent changes in relative importance of different aerosol emissions. The less stringent scenarios (UNEP BASE and UNEP SLCP) result in negative aerosol radiative forcing across sub-Saharan Africa due to higher concentrations of particularly scattering aerosol. In particular, the UNEP SLCP scenario targets BC, resulting in flat or decreasing BC emission profiles, depending on sub-region, from the baseline to near future, but has nearly the same SO<sub>2</sub> increase as in UNEP Base. Hence, the negative radiative forcing is therefore nearly as strong in UNEP SLCP as in UNEP BASE. Although the cooling by SO<sub>2</sub> offsets a portion of the warming caused by greenhouse gases, the adverse health effects in UNEP BASE and UNEP SLCP scenarios due to poor air quality cannot be ignored. As expected, the more stringent scenarios (ECL6 SDS and ECL6 MFR) result in stronger positive aerosol-induced radiative forcing, thus contributing to warming but with reduced health risks due to improved air quality (Chalmers et al., 2012; Lund et al., 2019; Westervelt et al., 2017; Zhang et al., 2025).

565

570

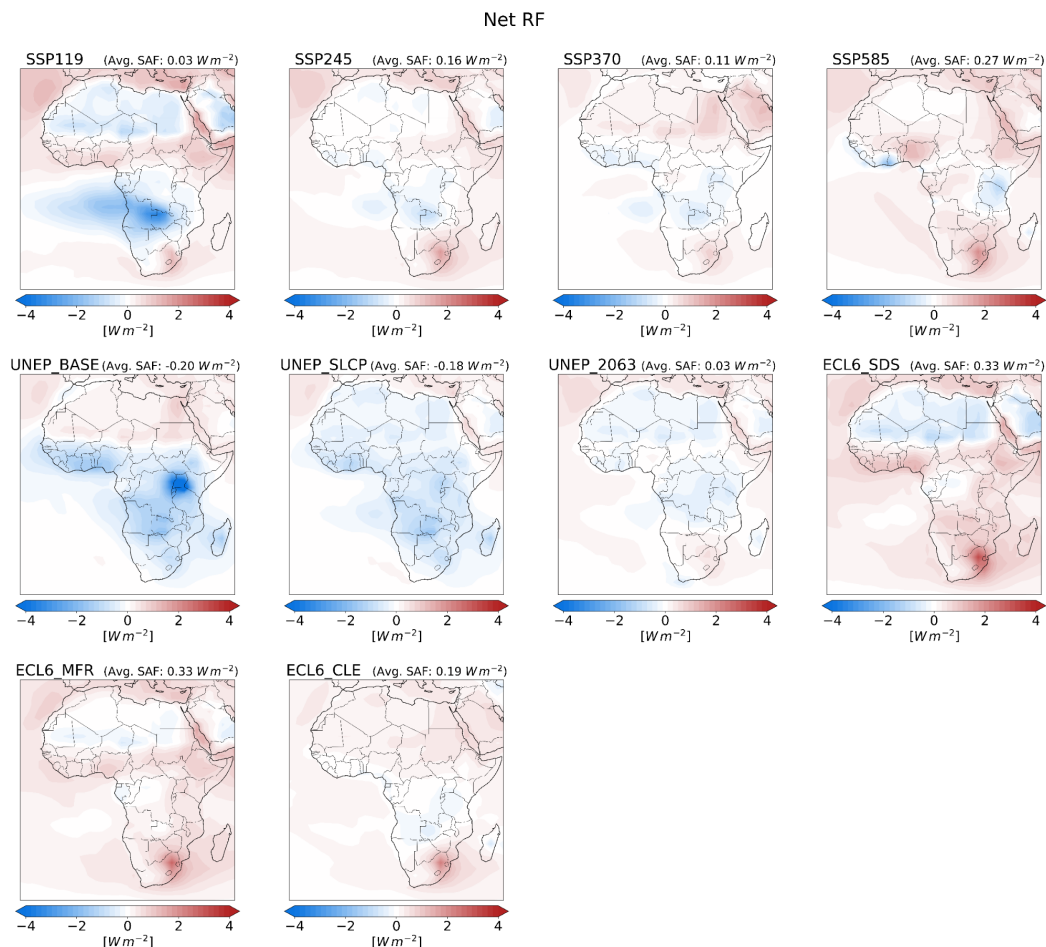


**Figure 8:** Net aerosol-induced radiative forcing estimated due to changes in emissions between 2050 and baseline.

#### 4. Discussion

Emissions of aerosol species across sub-Saharan Africa show substantial variability in existing inventories and over time, influenced by both regional factors and scenario-specific dynamics. The scenarios are designed to have large spread, reflecting uncertainties in how African nations will develop and lack of detailed assumptions. But there is also significant spread between the scenarios that assume weak or strong air pollution mitigation. The recent emission inventories differ and often lack up-to-date baselines (CEDS is not updated to 2022 and is not harmonized with scenarios); there is the need for improved data to enhance inventory construction and reduce uncertainties. For instance, BC emissions show variability throughout the historical period, but SO<sub>2</sub> emissions exhibit more consistency between inventories, particularly in



recent years, where “real-world” emissions track the high projections. The large spread and regional heterogeneity in projected air pollution emissions are consistent with findings from previous studies (Keita et al., 2021; Shindell et al., 2022). For example, Shindell et al. (2022) highlight that Southern Africa is projected to have the highest SO<sub>2</sub> emissions from power plants in the industrial sector, while Western and Eastern Africa are expected to see the largest BC emissions, primarily from the residential sector, under the high-emission SSP370 scenario, by mid-century. Additionally, Bonjour et al. (2013) and Chowdhury et al. (2023), noted that over 90 % of households in sub-Saharan Africa rely on solid fuels for cooking and domestic activities, further emphasizing the dominant role of the residential sector in BC emissions across all scenarios for the region.

Sub-Saharan Africa is undergoing two major simultaneous transformations: a shift from traditional to modern sources of environmental pollution and a significant change in the disease burden, moving from communicable to non-communicable diseases (Bigna and Noubiap, 2019). Despite these shifts, household air pollution (HAP) continues to contribute to over 70 % of anthropogenic PM<sub>2.5</sub> emissions in the region (McDuffie et al., 2020). Although HAP is gradually decreasing in certain areas as households transition to cleaner alternatives (Bescond et al., 2019), the pace is inconsistent across the continent. Notably, Northern Africa stands out as the sub-region with the least emissions from the residential sector, attributed to greater adoption of LPG for household activities.

Our findings on population-weighted PM<sub>2.5</sub> exposure align with those of Shindell et al. (2022), who observed that increases in PM<sub>2.5</sub> exposure under the SSP370 scenario are notably large for East, Northern, and West Africa, while being relatively modest in Central and Southern Africa. The variation in national-level PM<sub>2.5</sub> exposure across the African region is also evident, with significant increases observed in countries such as Nigeria, Egypt, Ethiopia, Uganda, Rwanda, and Burundi under the SSP370 scenario. Shindell et al. (2022) study was conducted using only the SSPs, with emphasis on the SSP119 and SSP370 scenarios, whereas our study expanded upon this by including a broader set of scenarios, including SSPs, ECLIPSE, and UNEP scenarios, to explore a diverse set of future possibilities under plausible conditions. Similarly, Wells et al. (2024) study using only the SSPs identified elevated PM<sub>2.5</sub> exposure levels across tropical regions of Africa. Furthermore, Chowdhury et al. (2020, 2022) found that Nigeria exhibits the highest PM<sub>2.5</sub> exposure levels in West Africa.

Shindell et al. (2022) found that, under the SSP119 scenario, annual premature deaths due to PM<sub>2.5</sub> are projected to decrease by approximately 515,000 by 2050, compared to the SSP370 scenario, with reductions of 100,000, 175,000, 55,000, 140,000, and 45,000 in Northern, West, Central, East, and Southern Africa, respectively. Wells et al. (2024) estimate that if Africa follows the high-emission SSP370 pathway instead of the low-emission SSP119 pathway, there could be approximately 150,000 additional deaths per year from PM<sub>2.5</sub> exposure. The implementation of the strictest emission reductions could have a substantial positive impact on public health outcomes but would still result in several hundred thousand excess deaths in the most populated regions. Pai et al. (2022) found that, even under an extreme abatement scenario with no anthropogenic emissions, more than half of the world’s population would still experience annual PM<sub>2.5</sub> exposures above the 5 µg m<sup>-3</sup> guideline, including over 70 % of the African population and more than 60 % of the Asian population. This is largely due to natural sources such as fires and dust, which aligns with our findings.



Several global studies have explored future aerosol-induced radiative forcing and climate impacts using SSPs (Lund et al., 2019) and Representative Concentration Pathway (RCP) projections (Chalmers et al., 2012; Gillett and Von Salzen, 2013; Westervelt et al., 2015). While present-day and future radiative forcing estimates vary across studies, a consistent finding is the significant weakening of aerosol radiative forcing by 2100 across all scenarios (Lund et al., 2019). Chalmers et al. (2012) and Gillett and Von Salzen (2013) also investigated whether the rapid decline in aerosol emissions could lead to near-term warming. For instance, Chalmers et al. (2012) observed higher near-term warming in RCP2.6 compared to RCP4.5, despite lower greenhouse gas forcing in the former, highlighting the role of decreasing aerosol emissions. In contrast, Gillett and Von Salzen (2013) found no evidence of accelerated near-term warming linked to reduced aerosol emissions, underscoring the variability in model responses to aerosol changes. While these previous studies primarily focused on global trends, and the dynamics of aerosol-induced radiative forcing may vary regionally, particularly in Africa, they provide crucial insights into how aerosol radiative forcing evolves over time, particularly in response to changes in aerosol emissions.

Although our study does not consider the impacts of aerosols on atmospheric circulation and precipitation, prior research highlights their significant influence. For instance, Myhre et al. (2017) found that BC absorbs short-wave radiation, warming the atmosphere and potentially causing contrasting effects on circulation patterns and regional precipitation. Shindell et al. (2023) highlighted that Africa could significantly mitigate rainfall declines by implementing the ECL6 SDS scenario, which focuses on transitioning away from fossil fuels and minimizing food waste. Even though these changes may lead to modest near-term warming due to reduced aerosols, they offer long-term climate benefits.

Shindell et al. (2023) also noted that under the high-emission UNEP Baseline scenario, significant drought is projected in the Sahel, whereas implementing the Agenda 2063 scenario could prevent this drying and potentially lead to a slight increase in precipitation. Previous studies have shown that local reductions in African anthropogenic aerosol emissions significantly influence the West African Monsoon (WAM) and Sahel summer precipitation (Hirasawa et al., 2022; Shindell et al., 2023; Wells et al., 2023; Westervelt et al., 2018). However, the considerable uncertainty in aerosol emissions over northern Africa continues to contribute to the challenges in projecting Sahel precipitation changes in the near future (Monerie et al., 2023; Shindell et al., 2023; Toolan et al., 2024).

## 5. Conclusion

In this paper, we examined the wide range and regional heterogeneity in projected air pollution emissions in sub-Saharan Africa. We explored sub-regional and sectoral contributions to air pollution emissions in ECLIPSE, SSPs and UNEP scenarios identifying sectoral changes that influence air quality across Africa's regions. We estimated the difference in simulated population-weighted PM<sub>2.5</sub> exposure as well as continental and regional annual mean changes in PM<sub>2.5</sub> concentrations in 2050 relative to the baseline. Furthermore, we estimated the excess mortality associated with PM<sub>2.5</sub> exposure based on the baseline and projected 2050 emissions for each scenario. Lastly, we calculated radiative forcing due to changes in emissions between 2050 and baseline.



675 Using the ECLIPSE, SSPs, and UNEP emission projections, we find substantial sub-  
regional differences in BC, SO<sub>2</sub>, OC, and NO<sub>x</sub> emissions across sub-Saharan Africa. Emissions  
vary substantially depending on the scenario and region, with high emissions of BC, OC, and NO<sub>x</sub>  
680 in Western Africa, Eastern Africa, and Central Africa, and high emissions of SO<sub>2</sub> in Southern  
Africa. Key sectoral contributors to air pollution vary by region, with the residential, industrial,  
transportation, and energy sectors playing dominant roles depending on the region and scenario.  
In the baseline and by 2050, the residential sector will remain the largest source of BC emissions  
in sub-Saharan Africa, while in Northern Africa, the transportation sector leads. Sectoral emission  
distributions differ across SSPs, ECL6, and UNEP scenarios due to varying assumptions about  
685 regulations, technology, and economic development. Better and more spatially resolved  
assumptions about policy, technology, and economic development is needed for projections on  
the continent, especially for the upcoming IPCC AR7.

Regionally-averaged annual-mean PM<sub>2.5</sub> concentrations exhibit distinct trends across  
different sub-Saharan African regions, with variations driven by the stringency of emission  
690 scenarios. We find that regionally-averaged annual-mean population-weighted PM<sub>2.5</sub>  
concentrations are projected to increase by up to 6 µg m<sup>-3</sup> (37 %, SD ± 2.7 µg m<sup>-3</sup>) under the  
UNEP Baseline, SSP370, and ECL6 CLE scenarios by 2050, when averaged across the African  
continent. Conversely, decreases of up to 5 µg m<sup>-3</sup> (8 %, SD ± 2.5 µg m<sup>-3</sup>) in Western Africa and  
3 µg m<sup>-3</sup> (39 %, SD ± 1.4 µg m<sup>-3</sup>) in Southern Africa are projected under the ECL6 SDS and MFR  
695 scenarios. Western, Eastern, and Northern Africa are projected to experience the highest  
exposure levels under the UNEP Baseline, SSP370, and ECL6 CLE scenarios, driven by  
increased emissions from the residential, industrial, transportation, and energy sectors. In  
contrast, Southern Africa is projected to see declines in annual PM<sub>2.5</sub> levels under the SSP370  
and ECL6 CLE scenarios, with reductions of 0.6 µg m<sup>-3</sup> (6 %) and 0.3 µg m<sup>-3</sup> (3 %), respectively,  
700 primarily due to decreased emissions from the energy and industrial sectors. By 2050, annual-  
mean PM<sub>2.5</sub> concentrations for sub-Saharan Africa differ by up to a factor of 2 between the highest  
emission scenario (UNEP Baseline) and the lowest (SSP119) when averaged across the  
continent, further highlighting a substantial spread in future emission projections.

705 Substantial increases in excess deaths due to PM<sub>2.5</sub> are projected in almost all scenarios,  
largely driven by significant population growth. We find that by 2050, Western Africa is projected  
to experience the highest increase in excess deaths across all scenarios, with an increase of over  
2.5 times compared to the baseline under the SSP370 and UNEP Baseline scenarios, driven  
primarily by population growth and aging. Eastern, Northern, Central, and Southern Africa follow  
710 in terms of projected excess deaths, but Southern Africa is projected to have the smallest  
increase, remaining below 0.05 million. While PM<sub>2.5</sub> reductions may slightly decrease mortality in  
some areas, population growth will still lead to hundreds of thousands of excess deaths,  
underscoring the need for significant PM<sub>2.5</sub> reductions. Epidemiological and pollution transitions  
are projected to reduce excess deaths in all regions, particularly in Western, Southern, and  
715 Northern Africa, with notable reductions in Southern Africa under certain scenarios.

We find a net positive aerosol-induced forcing across sub-Saharan Africa in all scenarios,  
by 2050 except UNEP BASE and UNEP SLCP, with values ranging from 0.03 W m<sup>-2</sup> in SSP119  
to 0.27 W m<sup>-2</sup> in SSP585, driven mainly by changes in scattering aerosols. Regional patterns  
720 show both positive and negative aerosol forcing depending on the scenario, with Southern Africa  
experiencing warming in all but two scenarios (UNEP BASE and UNEP SLCP) due to reductions  
in industrial emissions. The less stringent scenarios (UNEP BASE and UNEP SLCP) lead to



negative aerosol radiative forcing across Sub-Saharan Africa, primarily due to higher scattering aerosol concentrations, with UNEP SLCP focusing on eliminating BC emissions but with no changes to SO<sub>2</sub> emissions. Further work is needed to quantify the associated climate implications and risks.

This work provides profound insights into Africa's complex and diverse emissions landscape and lays the groundwork for future research and policy interventions. Understanding the drivers of change and the spread in scenarios is critical for addressing future emissions and their impacts. Differences in emissions projections highlight the need for robust analysis of socio-economic, regulatory, and technological pathways. Additionally, improving present-day data is essential to better constrain the baseline for scenarios, ensuring that models accurately reflect current emissions and activity levels. Accurate activity data and harmonization efforts are especially essential for upcoming assessment efforts aimed at informing policy makers, such as the various elements of the 7th Assessment Report of the Intergovernmental Panel on Climate Change, which will rely on these baselines to effectively consider the implications of future climate and air quality policies.

#### **Code Availability**

The OsloCTM3 model is available from <https://github.com/NordicESMhub/OsloCTM3> (details about version used in the present study will be provided upon request to the corresponding author). The data analysis was conducted using Bash scripting and Python programming languages.

745

#### **Data Availability**

The OsloCTM3 model outputs are available here: <https://figshare.com/account/items/28030610/edit>. NASA data is accessible through: <https://www.earthdata.nasa.gov/>. Satellite-derived PM2.5 data is available <https://sites.wustl.edu/acag/datasets/surface-pm2-5/>.

The SSP scenarios are provided at <https://iiasa.ac.at/models-tools-data>, and baseline mortality data can be accessed through <https://vizhub.healthdata.org/gbd-results/>.

#### **Author Contributions**

MTL, BHS, DMW, SC, GM, ANJ, and JAA conceptualized and designed the study. MTL performed the OsloCTM3 simulations; ANJ processed and prepared emissions; GM performed the radiative forcing calculations; SC performed the health impact assessment calculations; JAA performed data analysis and led the writing; All authors reviewed and edited the paper.

#### **Competing Interests**

One author is a member of the editorial board of journal Atmospheric Chemistry and Physics.

#### **Acknowledgements**

The authors acknowledge funding from the Research Council of Norway. The authors acknowledge the UNINETT Sigma2 – the National Infrastructure for High-Performance Computing and Data Storage in Norway – resources (grant no. NN9188K). We also acknowledge support by the Center for Advanced Study in Oslo, Norway which funded and hosted the HETCLIF centre during the academic year of 2023/24.

This work was also supported by the National Science Foundation Office of International Science and Engineering (OISE) Award Number 2020677.



## References

- Abera, A., Friberg, J., Isaxon, C., Jerrett, M., Malmqvist, E., Sjöström, C., Taj, T., and Vargas, A. M.: Air Quality in Africa: Public Health Implications, *Annu Rev Public Health*, 42, 193–210, <https://doi.org/10.1146/ANNUREV-PUBLHEALTH-100119-113802/CITE/REFWORKS>, 2020.
- Albrecht, B. A.: Aerosols, Cloud Microphysics, and Fractional Cloudiness, *Science* (1979), 245, 1227–1230, <https://doi.org/10.1126/SCIENCE.245.4923.1227>, 1989.
- Amann, M., Bertok, I., Borken-Kleefeld, J., Cofala, J., Heyes, C., Höglund-Isaksson, L., Klimont, Z., Nguyen, B., Posch, M., Rafaj, P., Sandler, R., Schöpp, W., Wagner, F., and Winiwarer, W.: Cost-effective control of air quality and greenhouse gases in Europe: Modeling and policy applications, *Environmental Modelling & Software*, 26, 1489–1501, <https://doi.org/10.1016/J.ENVSOFT.2011.07.012>, 2011.
- Bauer, S. E., Im, U., Mezuman, K., and Gao, C. Y.: Desert Dust, Industrialization, and Agricultural Fires: Health Impacts of Outdoor Air Pollution in Africa, *Journal of Geophysical Research: Atmospheres*, 124, 4104–4120, <https://doi.org/10.1029/2018JD029336>, 2019.
- Bescond, D., Cole, W., Diez De Medina, R., Lame, R. G., Kucera, D., Kühn, S., Lee, S., Maitre, N., Mathys, Q., Morgan, M., Perardel, Y., Sodergren, M.-C., Vazquez-Alvarez, R., and Fuentes, M. V.: THE GLOBAL LABOUR INCOME SHARE AND DISTRIBUTION Data Production and Analysis Unit, ILO Department of Statistics Methodological description, 2019.
- Bigna, J. J. and Noubiap, J. J.: The rising burden of non-communicable diseases in sub-Saharan Africa, *Lancet Glob Health*, 7, e1295–e1296, [https://doi.org/10.1016/S2214-109X\(19\)30370-5](https://doi.org/10.1016/S2214-109X(19)30370-5), 2019.
- Bonjour, S., Adair-Rohani, H., Wolf, J., Bruce, N. G., Mehta, S., Prüss-Ustün, A., Lahiff, M., Rehfuess, E. A., Mishra, V., and Smith, K. R.: Solid fuel use for household cooking: Country and regional estimates for 1980–2010, *Environ Health Perspect*, 121, 784–790, [https://doi.org/10.1289/EHP.1205987/SUPPL\\_FILE/EHP.1205987.S001.PDF](https://doi.org/10.1289/EHP.1205987/SUPPL_FILE/EHP.1205987.S001.PDF), 2013.
- Burnett, R., Chen, H., Szyszkowicz, M., Fann, N., Hubbell, B., Pope, C. A., Apte, J. S., Brauer, M., Cohen, A., Weichenthal, S., Coggins, J., Di, Q., Brunekreef, B., Frostad, J., Lim, S. S., Kan, H., Walker, K. D., Thurston, G. D., Hayes, R. B., Lim, C. C., Turner, M. C., Jerrett, M., Krewski, D., Gapstur, S. M., Diver, W. R., Ostro, B., Goldberg, D., Crouse, D. L., Martin, R. V., Peters, P., Pinault, L., Tjepkema, M., Van Donkelaar, A., Villeneuve, P. J., Miller, A. B., Yin, P., Zhou, M., Wang, L., Janssen, N. A. H., Marra, M., Atkinson, R. W., Tsang, H., Thach, T. Q., Cannon, J. B., Allen, R. T., Hart, J. E., Laden, F., Cesaroni, G., Forastiere, F., Weinmayr, G., Jaensch, A., Nagel, G., Concin, H., and Spadaro, J. V.: Global estimates of mortality associated with longterm exposure to outdoor fine particulate matter, *Proc Natl Acad Sci U S A*, 115, 9592–9597, [https://doi.org/10.1073/PNAS.1803222115/SUPPL\\_FILE/PNAS.1803222115.SAPP.PDF](https://doi.org/10.1073/PNAS.1803222115/SUPPL_FILE/PNAS.1803222115.SAPP.PDF), 2018.
- Chalmers, N., Highwood, E. J., Hawkins, E., Sutton, R., and Wilcox, L. J.: Aerosol contribution to the rapid warming of near-term climate under RCP 2.6, *Geophys Res Lett*, 39, <https://doi.org/10.1029/2012GL052848>, 2012.



820 Chowdhury, S., Dey, S., Guttikunda, S., Pillarisetti, A., Smith, K. R., and Girolamo, L. Di: Indian annual ambient air quality standard is achievable by completely mitigating emissions from household sources, *Proc Natl Acad Sci U S A*, 166, 10711–10716, [https://doi.org/10.1073/PNAS.1900888116/SUPPL\\_FILE/PNAS.1900888116.SAPP.PDF](https://doi.org/10.1073/PNAS.1900888116/SUPPL_FILE/PNAS.1900888116.SAPP.PDF), 2019.

825 Chowdhury, S., Hänninen, R., Sofiev, M., and Aunan, K.: Fires as a source of annual ambient PM<sub>2.5</sub> exposure and chronic health impacts in Europe, *Science of The Total Environment*, 922, 171314, <https://doi.org/10.1016/J.SCITOTENV.2024.171314>, 2024.

830 Chowdhury, S., Pillarisetti, A., Oberholzer, A., Jetter, J., Mitchell, J., Cappuccilli, E., Aamaas, B., Aunan, K., Pozzer, A., and Alexander, D.: A global review of the state of the evidence of household air pollution's contribution to ambient fine particulate matter and their related health impacts, *Environ Int*, 173, 107835, <https://doi.org/10.1016/J.ENVINT.2023.107835>, 2023.

835 Chowdhury, S., Pozzer, A., Dey, S., Klingmueller, K., and Lelieveld, J.: Changing risk factors that contribute to premature mortality from ambient air pollution between 2000 and 2015, *Environmental Research Letters*, 15, 074010, <https://doi.org/10.1088/1748-9326/AB8334>, 2020.

840 Chowdhury, S., Pozzer, A., Haines, A., Klingmüller, K., Münzel, T., Paasonen, P., Sharma, A., Venkataraman, C., and Lelieveld, J.: Global health burden of ambient PM<sub>2.5</sub> and the contribution of anthropogenic black carbon and organic aerosols, *Environ Int*, 159, 107020, <https://doi.org/10.1016/J.ENVINT.2021.107020>, 2022.

845 Cohen, A. J., Brauer, M., Burnett, R., Anderson, H. R., Frostad, J., Estep, K., Balakrishnan, K., Brunekreef, B., Dandona, L., Dandona, R., Feigin, V., Freedman, G., Hubbell, B., Jobling, A., Kan, H., Knibbs, L., Liu, Y., Martin, R., Morawska, L., Pope, C. A., Shin, H., Straif, K., Shaddick, G., Thomas, M., van Dingenen, R., van Donkelaar, A., Vos, T., Murray, C. J. L., and Forouzanfar, M. H.: Estimates and 25-year trends of the global burden of disease attributable to ambient air pollution: an analysis of data from the Global Burden of Diseases Study 2015, *The Lancet*, 389, 1907–1918, [https://doi.org/10.1016/S0140-6736\(17\)30505-6](https://doi.org/10.1016/S0140-6736(17)30505-6), 2017.

850 Crippa, M., Guizzardi, D., Muntean, M., Schaaf, E., Dentener, F., Van Aardenne, J. A., Monni, S., Doering, U., Olivier, J. G. J., Pagliari, V., and Janssens-Maenhout, G.: Gridded emissions of air pollutants for the period 1970–2012 within EDGAR v4.3.2, *Earth Syst Sci Data*, 10, 1987–2013, <https://doi.org/10.5194/ESSD-10-1987-2018>, 2018.

855 Fontes, T., Li, P., Barros, N., and Zhao, P.: Trends of PM<sub>2.5</sub> concentrations in China: A long term approach, *J Environ Manage*, 196, 719–732, <https://doi.org/10.1016/J.JENVMAN.2017.03.074>, 2017.

GBD: <https://vizhub.healthdata.org/gbd-results/>, last access: 21 December 2024.

860 Gidden, M. J., Riahi, K., Smith, S. J., Fujimori, S., Luderer, G., Kriegler, E., Van Vuuren, D. P., Van Den Berg, M., Feng, L., Klein, D., Calvin, K., Doelman, J. C., Frank, S., Fricko, O., Harmsen, M., Hasegawa, T., Havlik, P., Hilaire, J., Hoesly, R., Horing, J., Popp, A., Stehfest, E., and Takahashi, K.: Global emissions pathways under different socioeconomic scenarios for use in CMIP6: A dataset of harmonized emissions trajectories through the end of the century, *Geosci Model Dev*, 12, 1443–1475, <https://doi.org/10.5194/GMD-12-1443-2019>, 2019.



- 870 Gillett, N. P. and Von Salzen, K.: The role of reduced aerosol precursor emissions in driving near-term warming, *Environmental Research Letters*, 8, 034008, <https://doi.org/10.1088/1748-9326/8/3/034008>, 2013.
- Hirasawa, H., Kushner, P. J., Sigmond, M., Fyfe, J., and Deser, C.: Evolving Sahel Rainfall Response to Anthropogenic Aerosols Driven by Shifting Regional Oceanic and Emission Influences, *J Clim*, 35, 3181–3193, <https://doi.org/10.1175/JCLI-D-21-0795.1>, 2022.
- 875 Hoesly, R. M., Smith, S. J., Feng, L., Klimont, Z., Janssens-Maenhout, G., Pitkanen, T., Seibert, J. J., Vu, L., Andres, R. J., Bolt, R. M., Bond, T. C., Dawidowski, L., Kholod, N., Kurokawa, J. I., Li, M., Liu, L., Lu, Z., Moura, M. C. P., O'Rourke, P. R., and Zhang, Q.: Historical (1750-2014) anthropogenic emissions of reactive gases and aerosols from the Community Emissions Data System (CEDS), *Geosci Model Dev*, 11, 369–408, <https://doi.org/10.5194/GMD-11-369-2018>,  
880 2018.
- IEA: Clean Energy Transitions in North Africa – Analysis - IEA, 2020.
- IIASA: <https://iiasa.ac.at/models-tools-data>, last access: 2 August 2024.
- 885 Janssens-Maenhout, G., Crippa, M., Guizzardi, D., Muntean, M., Schaaf, E., Dentener, F., Bergamaschi, P., Pagliari, V., Olivier, J. G. J., Peters, J. A. H. W., Van Aardenne, J. A., Monni, S., Doering, U., Roxana Petrescu, A. M., Solazzo, E., and Oreggioni, G. D.: EDGAR v4.3.2 Global Atlas of the three major greenhouse gas emissions for the period 1970-2012, *Earth Syst Sci Data*,  
890 11, 959–1002, <https://doi.org/10.5194/ESSD-11-959-2019>, 2019.
- Jones, B. and O'Neill, B. C.: Spatially explicit global population scenarios consistent with the Shared Socioeconomic Pathways, *Environmental Research Letters*, 11, 084003, <https://doi.org/10.1088/1748-9326/11/8/084003>, 2016.
- 895 Katoto, P. D. M. C., Byamungu, L., Brand, A. S., Mokaya, J., Strijdom, H., Goswami, N., De Boever, P., Nawrot, T. S., and Nemery, B.: Ambient air pollution and health in Sub-Saharan Africa: Current evidence, perspectives and a call to action., *Environ Res*, 173, 174–188, <https://doi.org/10.1016/J.ENVRES.2019.03.029>, 2019.
- 900 Keita, S., Liousse, C., Assamoi, E. M., Doumbia, T., N'Datchoh, E. T., Gnamien, S., Elguindi, N., Granier, C., and Yoboué, V.: African anthropogenic emissions inventory for gases and particles from 1990 to 2015, *Earth Syst Sci Data*, 13, 3691–3705, <https://doi.org/10.5194/ESSD-13-3691-2021>, 2021.
- 905 LEAP: LEAP: The Low Emissions Analysis Platform, 2021.
- Leibensperger, E. M., Mickley, L. J., Jacob, D. J., Chen, W. T., Seinfeld, J. H., Nenes, A., Adams, P. J., Streets, D. G., Kumar, N., and Rind, D.: Climatic effects of 1950-2050 changes in US anthropogenic aerosols-Part 1: Aerosol trends and radiative forcing, *Atmos Chem Phys*, 12, 3333–3348, <https://doi.org/10.5194/ACP-12-3333-2012>, 2012.
- 910



- 915 Lund, M. T., Myhre, G., and Samset, B. H.: Anthropogenic aerosol forcing under the Shared Socioeconomic Pathways, *Atmos Chem Phys*, 19, 13827–13839, <https://doi.org/10.5194/acp-19-13827-2019>, 2019.
- 920 Lund, M. T., Myhre, G., Skeie, R. B., Samset, B. H., and Klimont, Z.: Implications of differences between recent anthropogenic aerosol emission inventories for diagnosed AOD and radiative forcing from 1990 to 2019, *Atmos Chem Phys*, 23, 6647–6662, <https://doi.org/10.5194/ACP-23-6647-2023>, 2023.
- 925 Lund, M. T., Myhre, G., Søvde Haslerud, A., Bieltvedt Skeie, R., Griesfeller, J., Matthew Platt, S., Kumar, R., Lund Myhre, C., and Schulz, M.: Concentrations and radiative forcing of anthropogenic aerosols from 1750 to 2014 simulated with the Oslo CTM3 and CEDS emission inventory, *Geosci Model Dev*, 11, 4909–4931, <https://doi.org/10.5194/GMD-11-4909-2018>, 2018.
- 930 McDuffie, E. E., Smith, S. J., O'Rourke, P., Tibrewal, K., Venkataraman, C., Marais, E. A., Zheng, B., Crippa, M., Brauer, M., and Martin, R. V.: A global anthropogenic emission inventory of atmospheric pollutants from sector- And fuel-specific sources (1970–2017): An application of the Community Emissions Data System (CEDS), *Earth Syst Sci Data*, 12, 3413–3442, <https://doi.org/10.5194/ESSD-12-3413-2020>, 2020.
- 935 Monerie, P. A., Dittus, A. J., Wilcox, L. J., and Turner, A. G.: Uncertainty in Simulating Twentieth Century West African Precipitation Trends: The Role of Anthropogenic Aerosol Emissions, *Earths Future*, 11, e2022EF002995, <https://doi.org/10.1029/2022EF002995>, 2023.
- 940 Murray, C. J. L., Abbafati, C., Abbas, K. M., Abbasi-Kangevari, M., Abd-Allah, F., Abdelalim, A., Abdollahi, M., Abdollahpour, I., Abegaz, K. H., Abolhassani, H., Aboyans, V., Abreu, L. G., Abrigo, M. R. M., Abualhasan, A., Abu-Raddad, L. J., Abushouk, A. I., Adabi, M., Adekanmbi, V., Adeoye, A. M., Adetokunboh, O. O., Adham, D., Advani, S. M., Afshin, A., Agarwal, G., Aghamir, S. M. K., Agrawal, A., Ahmad, T., Ahmadi, K., Ahmadi, M., Ahmadi, H., Ahmed, M. B., Akalu, T. Y., Akinyemi, R. O., Akinyemiju, T., Akombi, B., Akunna, C. J., Alahdab, F., Al-Aly, Z., Alam, K., Alam, S., Alam, T., Alanezi, F. M., Alanzi, T. M., Alemu, B. W., Alhabib, K. F., Ali, M., Ali, S., Alicandro, G., Alinia, C., Alipour, V., Alizade, H., Aljunid, S. M., Alla, F., Allebeck, P., Almasi-Hashiani, A., Al-Mekhlafi, H. M., Alonso, J., Altirkawi, K. A., Amini-Rarani, M., Amiri, F., Amugsi, D. A., Ancuceanu, R., Anderlini, D., Anderson, J. A., Andrei, C. L., Andrei, T., Angus, C., Anjomshoa, M., Ansari, F., Ansari-Moghaddam, A., Antonazzo, I. C., Antonio, C. A. T., Antony, C. M., Antriandarti, E., Anvari, D., Anwer, R., Appiah, S. C. Y., Arabloo, J., Arab-Zozani, M., Aravkin, A. Y., Ariani, F., Armoon, B., Ärnlöv, J., Arzani, A., Asadi-Aliabadi, M., Asadi-Pooya, A. A., Ashbaugh, C., Assmus, M., Atafar, Z., Atnafu, D. D., Atout, M. M. d. W., Ausloos, F., Ausloos, M., Ayala Quintanilla, B. P., Ayano, G., Ayanore, M. A., Azari, S., Azarian, G., Azene, Z. N., et al.: Global burden of 87 risk factors in 204 countries and territories, 1990–2019: a systematic analysis for the Global Burden of Disease Study 2019, *Lancet*, 396, 1223–1249, [https://doi.org/10.1016/S0140-6736\(20\)30752-2](https://doi.org/10.1016/S0140-6736(20)30752-2), 2020.
- 955 Myhre, G., Aas, W., Cherian, R., Collins, W., Faluvegi, G., Flanner, M., Forster, P., Hodnebrog, Ø., Klimont, Z., Lund, M. T., Mülmenstädt, J., Lund Myhre, C., Olivé, D., Prather, M., Quaas, J., Samset, B. H., Schnell, J. L., Schulz, M., Shindell, D., Skeie, R. B., Takemura, T., and Tsyro, S.: Multi-model simulations of aerosol and ozone radiative forcing due to anthropogenic emission



- 960 changes during the period 1990–2015, *Atmos Chem Phys*, 17, 2709–2720,  
<https://doi.org/10.5194/ACP-17-2709-2017>, 2017.
- Myhre, G., Samset, B. H., Schulz, M., Balkanski, Y., Bauer, S., Bernsten, T. K., Bian, H., Bellouin, N., Chin, M., Diehl, T., Easter, R. C., Feichter, J., Ghan, S. J., Hauglustaine, D., Iversen, T., Kinne, S., Kirkevåg, A., Lamarque, J. F., Lin, G., Liu, X., Lund, M. T., Luo, G., Ma, X., Van Noije, T., Penner, J. E., Rasch, P. J., Ruiz, A., Seland, Skeie, R. B., Stier, P., Takemura, T., Tsigaridis, K., Wang, P., Wang, Z., Xu, L., Yu, H., Yu, F., Yoon, J. H., Zhang, K., Zhang, H., and Zhou, C.: Radiative forcing of the direct aerosol effect from AeroCom Phase II simulations, *Atmos Chem Phys*, 13, 1853–1877, <https://doi.org/10.5194/ACP-13-1853-2013>, 2013.
- 970 O'Neill, B. C., Kriegler, E., Ebi, K. L., Kemp-Benedict, E., Riahi, K., Rothman, D. S., van Ruijven, B. J., van Vuuren, D. P., Birkmann, J., Kok, K., Levy, M., and Solecki, W.: The roads ahead: Narratives for shared socioeconomic pathways describing world futures in the 21st century, *Global Environmental Change*, 42, 169–180,  
975 <https://doi.org/10.1016/J.GLOENVCHA.2015.01.004>, 2017.
- Pai, S. J., Carter, T. S., Heald, C. L., and Kroll, J. H.: Updated World Health Organization Air Quality Guidelines Highlight the Importance of Non-anthropogenic PM<sub>2.5</sub>, *Environ Sci Technol Lett*, 9, 501–506,  
980 <https://doi.org/10.1021/ACS.ESTLETT.2C00203>/ASSET/IMAGES/LARGE/EZ2C00203\_0003.JPG, 2022.
- Platnick, S., P. H. K. M. and M. D. K.: MODIS Atmosphere L3 Daily Product. NASA MODIS Adaptive Processing System, Goddard Space Flight Center, USA,  
985 [https://doi.org/http://dx.doi.org/10.5067/MODIS/MOD08\\_D3.061](https://doi.org/http://dx.doi.org/10.5067/MODIS/MOD08_D3.061), 2015.
- Pozzer, A., Anenberg, S. C., Dey, S., Haines, A., Lelieveld, J., and Chowdhury, S.: Mortality Attributable to Ambient Air Pollution: A Review of Global Estimates, *Geohealth*, 7, e2022GH000711, <https://doi.org/10.1029/2022GH000711>, 2023.
- 990 Quaas, J., Boucher, O., and Lohmann, U.: Atmospheric Chemistry and Physics Constraining the total aerosol indirect effect in the LMDZ and ECHAM4 GCMs using MODIS satellite data, *Atmos. Chem. Phys*, 6, 947–955, <https://doi.org/10.5194/WDCC/MODIS>, 2006.
- 995 Rao, S., Klimont, Z., Smith, S. J., Van Dingenen, R., Dentener, F., Bouwman, L., Riahi, K., Amann, M., Bodirsky, B. L., van Vuuren, D. P., Aleluia Reis, L., Calvin, K., Drouet, L., Fricko, O., Fujimori, S., Gernaat, D., Havlik, P., Harmsen, M., Hasegawa, T., Heyes, C., Hilaire, J., Luderer, G., Masui, T., Stehfest, E., Strefler, J., van der Sluis, S., and Tavoni, M.: Future air pollution in the Shared Socio-economic Pathways, *Global Environmental Change*, 42, 346–358,  
1000 <https://doi.org/10.1016/J.GLOENVCHA.2016.05.012>, 2017.
- 1005 Riahi, K., van Vuuren, D. P., Kriegler, E., Edmonds, J., O'Neill, B. C., Fujimori, S., Bauer, N., Calvin, K., Dellink, R., Fricko, O., Lutz, W., Popp, A., Cuaserna, J. C., KC, S., Leimbach, M., Jiang, L., Kram, T., Rao, S., Emmerling, J., Ebi, K., Hasegawa, T., Havlik, P., Humpenöder, F., Da Silva, L. A., Smith, S., Stehfest, E., Bosetti, V., Eom, J., Gernaat, D., Masui, T., Rogelj, J., Strefler, J., Drouet, L., Krey, V., Luderer, G., Harmsen, M., Takahashi, K., Baumstark, L., Doelman, J. C., Kainuma, M., Klimont, Z., Marangoni, G., Lotze-Campen, H., Obersteiner, M.,



- 1010 Tabeau, A., and Tavoni, M.: The Shared Socioeconomic Pathways and their energy, land use, and greenhouse gas emissions implications: An overview, *Global Environmental Change*, 42, 153–168, <https://doi.org/10.1016/J.GLOENVCHA.2016.05.009>, 2017.
- 1015 Samset, B. H., Lund, M. T., Bollasina, M., Myhre, G., and Wilcox, L.: Emerging Asian aerosol patterns, *Nature Geoscience* 2019 12:8, 12, 582–584, <https://doi.org/10.1038/s41561-019-0424-5>, 2019.
- Samset, B. H., Sand, M., Smith, C. J., Bauer, S. E., Forster, P. M., Fuglestad, J. S., Osprey, S., and Schleussner, C. F.: Climate Impacts From a Removal of Anthropogenic Aerosol Emissions, *Geophys Res Lett*, 45, 1020–1029, <https://doi.org/10.1002/2017GL076079>, 2018.
- 1020 Shindell, D., Faluvegi, G., Parsons, L., Nagamoto, E., and Chang, J.: Premature Deaths in Africa Due To Particulate Matter Under High and Low Warming Scenarios, *Geohealth*, 6, e2022GH000601, <https://doi.org/10.1029/2022GH000601>, 2022.
- 1025 Shindell, D., Parsons, L., Faluvegi, G., Hicks, K., Kuylensstierna, J., and Heaps, C.: The important role of African emissions reductions in projected local rainfall changes, *NPJ Clim Atmos Sci*, 6, <https://doi.org/10.1038/s41612-023-00382-7>, 2023.
- 1030 Southerland, V. A., Brauer, M., Mohegh, A., Hammer, M. S., van Donkelaar, A., Martin, R. V., Apte, J. S., and Anenberg, S. C.: Global urban temporal trends in fine particulate matter (PM<sub>2.5</sub>) and attributable health burdens: estimates from global datasets, *Lancet Planet Health*, 6, e139–e146, [https://doi.org/10.1016/S2542-5196\(21\)00350-8](https://doi.org/10.1016/S2542-5196(21)00350-8), 2022.
- 1035 Søvde, O. A., Prather, M. J., Isaksen, I. S. A., Bernsten, T. K., Stordal, F., Zhu, X., Holmes, C. D., and Hsu, J.: The chemical transport model Oslo CTM3, *Geosci Model Dev*, 5, 1441–1469, <https://doi.org/10.5194/GMD-5-1441-2012>, 2012.
- 1040 Stamnes, K., Jayaweera, K., Tsay, S.-C., and Wiscombe, W.: Numerically stable algorithm for discrete-ordinate-method radiative transfer in multiple scattering and emitting layered media, *Applied Optics*, Vol. 27, Issue 12, pp. 2502–2509, 27, 2502–2509, <https://doi.org/10.1364/AO.27.002502>, 1988.
- 1045 Stjern, C. W., Samset, B. H., Myhre, G., Bian, H., Chin, M., Davila, Y., Dentener, F., Emmons, L., Flemming, J., Haslerud, A. S., Henze, D., Jonson, J. E., Kucsera, T., Lund, M. T., Schulz, M., Sudo, K., Takemura, T., and Tilmes, S.: Global and regional radiative forcing from 20 % reductions in BC, OC and SO<sub>4</sub> - An HTAP2 multi-model study, *Atmos Chem Phys*, 16, 13579–13599, <https://doi.org/10.5194/ACP-16-13579-2016>, 2016.
- 1050 Toolan, C. A., Amooli, J. A., Wilcox, L. J., Samset, B. H., Turner, A. G., and Westervelt, D. M.: Strong inter-model differences and biases in CMIP6 simulations of PM<sub>2.5</sub>, aerosol optical depth, and precipitation over Africa, <https://doi.org/10.5194/EGUSPHERE-2024-3057>, 2024.
- Turnock, S. T., Allen, R. J., Andrews, M., Bauer, S. E., Deushi, M., Emmons, L., Good, P., Horowitz, L., John, J. G., Michou, M., Nabat, P., Naik, V., Neubauer, D., O'Connor, F. M., Olivieri, D., Oshima, N., Schulz, M., Sellar, A., Shim, S., Takemura, T., Tilmes, S., Tsigaridis, K., Wu, T.,



- 1055 and Zhang, J.: Historical and future changes in air pollutants from CMIP6 models, *Atmos Chem Phys*, 20, 14547–14579, <https://doi.org/10.5194/ACP-20-14547-2020>, 2020.
- Twomey and S.: The Influence of Pollution on the Shortwave Albedo of Clouds., *JAtS*, 34, 1149–1154, [https://doi.org/10.1175/1520-0469\(1977\)034](https://doi.org/10.1175/1520-0469(1977)034), 1977.
- 1060 U.S. EPA: <https://www.airnow.gov/international/us-embassies-and-consulates/>, last access: 5 February 2024.
- 1065 UNEP: Integrated Assessment of Air Pollution and Climate Change for Sustainable Development in Africa - Summary for Decision Makers, 2022.
- Van Donkelaar, A., Hammer, M. S., Bindle, L., Brauer, M., Brook, J. R., Garay, M. J., Hsu, N. C., Kalashnikova, O. V., Kahn, R. A., Lee, C., Levy, R. C., Lyapustin, A., Sayer, A. M., and Martin, R. V.: Monthly Global Estimates of Fine Particulate Matter and Their Uncertainty, *Environ Sci Technol*, 55, 15287–15300, [https://doi.org/10.1021/ACS.EST.1C05309/ASSET/IMAGES/LARGE/ES1C05309\\_0007.JPEG](https://doi.org/10.1021/ACS.EST.1C05309/ASSET/IMAGES/LARGE/ES1C05309_0007.JPEG), 2021.
- 1070 Wang, P., Yang, Y., Xue, D., Ren, L., Tang, J., Leung, L. R., and Liao, H.: Aerosols overtake greenhouse gases causing a warmer climate and more weather extremes toward carbon neutrality, *Nature Communications* 2023 14:1, 14, 1–11, <https://doi.org/10.1038/s41467-023-42891-2>, 2023.
- 1075 Wells, C. D., Kasoar, M., Bellouin, N., and Voulgarakis, A.: Local and remote climate impacts of future African aerosol emissions, *Atmos Chem Phys*, 23, 3575–3593, <https://doi.org/10.5194/ACP-23-3575-2023>, 2023.
- 1080 Wells, C. D., Kasoar, M., Ezzati, M., and Voulgarakis, A.: Significant human health co-benefits of mitigating African emissions, *Atmos Chem Phys*, 24, 1025–1039, <https://doi.org/10.5194/ACP-24-1025-2024>, 2024.
- 1085 Westervelt, D. M., Conley, A. J., Fiore, A. M., Lamarque, J. F., Shindell, D., Previdi, M., Faluvegi, G., Correa, G., and Horowitz, L. W.: Multimodel precipitation responses to removal of U.S. sulfur dioxide emissions, *Journal of Geophysical Research: Atmospheres*, 122, 5024–5038, <https://doi.org/10.1002/2017JD026756>, 2017.
- 1090 Westervelt, D. M., Conley, A. J., Fiore, A. M., Lamarque, J. F., Shindell, D. T., Previdi, M., Mascioli, N. R., Faluvegi, G., Correa, G., and Horowitz, L. W.: Connecting regional aerosol emissions reductions to local and remote precipitation responses, *Atmos Chem Phys*, 18, 12461–12475, <https://doi.org/10.5194/ACP-18-12461-2018>, 2018.
- 1095 Westervelt, D. M., Horowitz, L. W., Naik, V., Golaz, J. C., and Mauzerall, D. L.: Radiative forcing and climate response to projected 21st century aerosol decreases, *Atmos Chem Phys*, 15, 12681–12703, <https://doi.org/10.5194/ACP-15-12681-2015>, 2015.
- 1100 Westervelt, D. M., Mascioli, N. R., Fiore, A. M., Conley, A. J., Lamarque, J. F., Shindell, D. T., Faluvegi, G., Previdi, M., Correa, G., and Horowitz, L. W.: Local and remote mean and extreme



- 1105 temperature response to regional aerosol emissions reductions, *Atmos Chem Phys*, 20, 3009–3027, <https://doi.org/10.5194/ACP-20-3009-2020>, 2020.
- WHO: <https://www.who.int/countries/>, last access: 21 December 2024.
- 1110 Yang, F., Lodder, P., Huang, N., Liu, X., Fu, M., and Guo, J.: Thirty-year trends of depressive disorders in 204 countries and territories from 1990 to 2019: An age-period-cohort analysis, *Psychiatry Res*, 328, 115433, <https://doi.org/10.1016/J.PSYCHRES.2023.115433>, 2023.
- 1115 Zhang, J., Chen, Y.-S., Gryspeerdt, E., Yamaguchi, T., and Feingold, G.: Radiative forcing from the 2020 shipping fuel regulation is large but hard to detect, *Communications Earth & Environment* 2025 6:1, 6, 1–11, <https://doi.org/10.1038/s43247-024-01911-9>, 2025.